

THE *DROSOPHILA* SMALL CONDUCTANCE CALCIUM-ACTIVATED
POTASSIUM CHANNEL GENE

by

André F. Rivard

A DISSERTATION

Presented to the Department of Neuroscience
and the Oregon Health & Science University

School of Medicine

in partial fulfillment of

the requirements for the degree of

Doctor of Philosophy

March 2007

School of Medicine
Oregon Health & Science University

CERTIFICATE OF APPROVAL

This is to certify that the Ph.D. dissertation of
André F. Rivard
has been approved



Mentor/Advisor


Member


Member


Member

Table of Contents

Acknowledgments	ii
Abstract	iii
List of Figures	iv
Abbreviations	v
Chapter I. Introduction	1
1. A Brief History	1
2. Potassium Channel Phylogeny	6
3. Mammalian SK Channels	13
4. <i>Drosophila</i> SK	19
Chapter II. Methods	21
Chapter III. Results	27
Chapter IV. Discussion	43
Chapter V. Summary and Conclusions	56
Bibliography	59
Appendix	84

Acknowledgments

I would like to thank my advisor John Adelman for his scientific guidance and personal friendship. The skill set that I have learned in his laboratory is broad and varied, reflecting his style or research. Mostly I am grateful for his patience during the difficult, trying thesis process. I hope to repay his commitment to my education by making significant contributions to the scientific community and society in general.

I would also like to thank the members of my thesis committee: James Maylie, Richard Walker, and Peter Gillespie. They, along with John, have picked me up when I have stumbled through this process. Scientifically I could not have imagined a better group of mentors.

I would like to thank all of the members of the Adelman and Maylie labs that I have interacted with during my tenure. Lab members tend to mirror the all of the exceptional attributes of the mentors that attract them.

On a personal note, I would like to thank my girlfriend Zara Patel for her love. I would like to thank my mother Betsy Rivard for being strong and raising three children on her own. My littermates, Kevin and Sarah, have also helped me through this process by setting a high standard for the family name.

Abstract

Drosophila contains one SK channel gene that is most similar to mammalian SK1. As with rodent SK1, traditional characterization attempts have proven difficult. When expressed in heterologous systems, dSK does not reach the cell surface. Chimeras containing the N and C termini of rat SK2 the transmembrane regions of dSK are TEA sensitive and apamin insensitive. Northern blots show that there are two transcripts. The transcripts, as determined by quantitative PCR, are developmentally regulated, with the highest levels of expression found in adult head. SK null flies generated by gamma ray deletion have no overt phenotype.

List of Figures

Figure 1. Dendrogram of the potassium channel superfamily

Figure 2. Potassium channel pore structures

Figure 3. CaMBD structure

Figure 4. SK sequence alignment

Figure 5. dSK gene cartoon

Figure 6. Mating scheme and polytene squash

Figure 7. RT-PCR on dSK null flies

Figure 8. Northern blot in dSK null Flies

Figure 9. Western blot with custom dSK antibodies

Figure 10. Quantitative PCR

Figure 11. dSK surface expression

Figure 12. Recordings of dSK chimeras

Figure 13. *Drosophila* S2 cells expression SK channels

Figure 14. Larval muscle recordings

Appendix Figure A. dSK cDNA cartoon showing location of antigen epitopes

Appendix Figure B. Full scale dSK gene cartoon showing two major splice variants

Abbreviations

¹²⁵I radioactive iodine with the atomic mass number 125

α -³²P-UTP uridine triphosphate with a radioactive phosphate (atomic mass number of 32) in the α position

ADAR adenosine deaminase RNA specific

AHP afterhyperpolarization

ATP adenosine triphosphate

BC before Christ

BK mammalian large conductance calcium-activated potassium channel (IUPAR K_{Ca}1.1)

BSA bovine serum albumin

°C degrees celsius

CA1 cornus amon region 1 of the hippocampus

Ca²⁺ divalent calcium ion

CaCl₂ calcium chloride

CaM calmodulin

CaMBD calmodulin binding domain

CamKII Ca²⁺/calmodulin dependent protein kinase II

cAMP cyclic adenosine monophosphate

CanB calcineurin B

Canton S the wild-type standard *Drosophila* strain, Canton Special

cDNA complimentary deoxyribonucleic acid

cGMP cyclic guanosine monophosphate

CHO Chinese hamster ovarian cells

CMV cytomegalovirus

Cos7 African green monkey kidney cell line

C-terminal towards the carboxy-terminus

DMEM Dulbeco's modified Eagle's medium

DNA deoxyribonucleic acid

dSK *Drosophila* small conductance calcium-activated potassium channel

Duke MSG Duke model systems genomics

Eag *ether-á-go-go*

EC50 the effective concentration that produces 50% of the maximal possible response

EDTA ethylenediamine tetraacetic acid

E-F hands a calcium binding protein structural motif

elk *ether-á-go-go like*

erg *ether-á-go-go related gene*

EST expressed sequence tag

GFP green fluorescent protein

HEPES 4-(2-hydroxyethyl)-1-piperazineethanesulfonic acid

I_A A-type (rapidly inactivating) potassium current of *Drosophila* muscle

I_{CF} the kinetically fast calcium activated potassium current of *Drosophila* muscle

I_{CS} the kinetically slow calcium activated potassium current of *Drosophila* muscle

IgG immunoglobulin G
I_K slowly activating, sustained potassium current of *Drosophila* muscle
IUPAR international union of pharmacology
[K⁺] monovalent potassium ion concentration
K⁺ monovalent potassium ion
kb kilo base
KCa1.1 a calcium-activated potassium channel
KCl potassium chloride
long-QT a heart syndrome characterized by a long interval between Q and T waves on an electrocardiogram
M ohms mega ohms
M-current non-inactivating potassium current
mg milli gram
Mg²⁺ divalent magnesium ion
μg micro gram
μl micro liter
μM micro molar
mM milli molar
MOPS 3-(N-morpholino)propanesulfonic acid
mRNA messenger ribonucleic acid
mSK mouse small conductance calcium-activated potassium channel
mV milli volt
myc a protein epitope tag
Na⁺ monovalent sodium ion
NaPO₄ sodium phosphate
nM nano molar
N-terminal towards the amino-terminus
P pore
PBS phosphate buffered saline
PCR polymerase chain reaction
PDZ a structural domain involved in protein-protein interactions
P-element parental element (a transposable element)
pH potenz hydrogen (inverse log of the hydrogen ion concentration)
pJPA plasmid John Peter Adelman
P-Loop pore loop
pS pico siemen
RACE rapid amplification of cDNA ends
RNA ribonucleic acid
RP49 ribosomal protein 49
rSK rat small conductance calcium-activated potassium channel
RT-PCR reverse transcription polymerase chain reaction
S2 Schneider 2 *Drosophila* cell line
S4 segment 4 (transmembrane segment four of a potassium channel, sometimes involved in voltage sensing)
SDS sodium dodecyl sulfate
SK small conductance calcium-activated potassium channel

SSC standard saline citrate buffer
TEA tetraethylammonium
TM transmembrane
UTR untranslated region
UV ultraviolet
V5 a protein epitope tag

Chapter I. Introduction

The foundations of modern neuroscience are strong and deep, precluding any thorough introductory discussion¹. There are, however, several specific, landmark discoveries that delineate a clear path from ignorance to our current understanding of small conductance calcium-activated potassium channels (SK channels). I have decided to begin this introduction with a brief description of these historical highlights. They will be followed by an account of mammalian *in vivo* SK research, discussing each of the relevant model systems. Next, our detailed knowledge of SK currents in mammalian systems will be contrasted with that which is known about *Drosophila* SK and other *Drosophila* potassium channels. Finally, I will end by listing the obvious holes in our current understanding of *Drosophila* SK, and the intriguing parallels to those in mammalian systems.

A Brief History

This history of bioelectricity rightly begins with a brief history of electricity. Historical reports of observed electrical phenomena are almost as old as history itself. Thales of Miletus, around 600 BC, observed that when a piece of amber was rubbed against animal fur, the fur and amber would attract human hair and particles of straw². In the 1600s the English scientist William Gilbert revisited the experiments of Thales and introduced the Latin term *electricus* from the Greek word for amber, *electron*³. Discovery of electrical phenomena eventually lead to

the manipulation of electrical phenomena by Pieter van Musschenbroek at the University of Leiden in 1745. He discovered how to store large quantities of static electricity in a capacitor-like device later called a Leyden jar⁴. Luigi Galvani eventually combined the separate studies of electricity and biomechanics in 1781. He observed that an electrostatic arc between the scalpel in his hand and the frog leg he was dissecting caused the frog leg to move⁵. The observed animation was faithfully repeated using electrostatic discharge from a Leyden jar. The specific conclusions that Galvani later drew from these observations turned out to be incorrect, but did not overshadow the importance of his discovery.

The notion that bioelectricity is ionic in nature came from the work of Sydney Ringer during the 1880s⁶. Ringer was trying to formulate a simplified perfusion solution that would support contractility in an isolated frog heart. He started with the observation that perfusion with blood would maintain contractility and so he decided to perfuse the heart with solutions containing some of the major known constituents of blood. The first perfusate he tried was a simple saline solution, and to his surprise contraction persisted. Upon a later attempt of the same experiment, however, the solution was no longer effective. It turns out that his assistant made the first perfusate using tap water, while he made the second solution using distilled water. Analysis of trace constituents in the tap water supplied by the New River Water Company showed that it contained calcium, potassium, magnesium, sodium, and chlorine. Furthermore he showed that the minimal constituents required to support contraction were the now famous ions of physiology, sodium, potassium, calcium, and chlorine. Somehow

Ringer's inorganic ions were required for bioelectrical phenomenon like those observed by Galvani.

These experiment showed that biomechanical processes were electrical in nature and required specific ions in solution. Scientists followed these observations with experiments designed to record and characterize observed electrical phenomena. The most significant advance towards this goal followed, as is the pattern, an advance in technology. Julius Bernstein created a device known as the differential rheotome⁷. This device had the time resolution necessary for recording rapid electrical events in nerves. Briefly, a spinning disc connects stimulating and recording circuits in an ordered fashion with adjustable, submillisecond resolution. Bernstein could take a temporal snapshot of the potential at any distance from the stimulating electrode. In 1868 he averaged many measurements and graphed voltage versus time for a fixed distance from the stimulus. This published image of "negative variation" was the first depiction of what is now recognized as the fundamental currency on the nervous system, the action potential⁸.

Hodgkin and Huxley elegantly described the underlying processes of the action potential that Bernstein observed, resulting in their seminal ionic theory of membrane excitation⁹. Most of the studies in the 1950s and 60s, the golden age of biophysics, took advantage of the large diameter of the squid giant axon. This preparation allowed scientists to control the potential across the cell membrane by inserting an axial electrode into the large diameter axon. By changing the concentration of Ringer's ions in intracellular and extracellular solutions, Hodgkin

and Huxley showed that the conductance changes were ionic in nature; furthermore extracellular sodium is required for membrane depolarization and intracellular potassium is required for membrane repolarization. Together with Bernard Katz, they were able to simulate the action potential trace with a kinetic model in which the permeability of the membrane to sodium and potassium changes over time¹⁰. The obvious question became, how does the membrane change its permeability to sodium and potassium? Two substances, tetrodotoxin and tetramethylammonium, helped scientists answer this question. The peptide toxin tetrodotoxin from the Fugu puffer fish was found to block sodium permeability changes in the squid giant axon¹¹, while tetramethylammonium blocked potassium permeability changes¹². This was the first suggestive evidence that separate receptors, or channels as they were now being called, were responsible for the ionic conductances described in the Hodgkin and Huxley model. Later studies would show that channel proteins span the membrane creating gated, aqueous pores through which ions can pass¹³.

The ion channels of the Hodgkin and Huxley model open in response to changes in voltage. The golden age of biophysics saw the discovery of several channels that are gated by molecules or ions, in current lexicon, ligand-gated channels. In fact, during this time period Gardos observed the first known member of the ligand-gated ion channel family central to this thesis¹⁴. In a set of straightforward experiments Gardos showed that calcium changed the potassium permeability of erythrocyte membranes. In the years that followed, calcium

activated potassium currents were discovered in diverse cell types, but were mainly found in neurons following action potential spikes.

The number and kind of “ion channels” reported in the literature began to grow, but strictly speaking they were new conductances, as ion channels were only a theory. In the early 1980s the laboratory of Shosaku Numa turned theory into reality by cloning the first ion channel¹⁵. The group used the electric organ of the torpedo ray as a highly enriched source of sodium channels. Tetrodotoxin selectively blocks this channel and its high affinity was exploited in their purification scheme. Proteins from a homogenate of torpedo ray electric organ that bound to immobilized tetrodotoxin were eluted and sequenced by Edman degradation. Small fragments of protein sequence from four identified subunits were used to make degenerate probes for cloning of the four separate genes.

The first cloned potassium channel gene was soon to follow. The Jan laboratory using a forward-genetic approach instead of biochemistry, cloned the *Shaker* channel gene in 1987¹⁶. The channel gets its name from a *Drosophila* mutant phenotype. *Shaker* flies literally shake as they recover from ether anesthesia¹⁷. Electrophysiological recordings from the flight muscle of these mutant flies reveal that they also lack a voltage-activated potassium conductance¹⁸. Through a labor-intensive process called gene walking (a technique that isolates successive overlapping genomic sequences), the exact location of the genetic lesion was found¹⁹. The sequence surrounding the lesion was used as probe in a screen of a wild-type cDNA library. Messenger RNA, reverse transcribed from full-length cloned cDNA, was injected into xenopus

oocytes. Several days later the oocytes expressed functional potassium channels on their surface membranes. The activity of the channels was recorded with glass microelectrodes in the two-electrode, voltage-clamp configuration. Isolation of channel cDNA sequence followed by expression of mRNA in xenopus oocytes became the model method for the discovery and study of new channel genes.

The laboratory of John Adelman cloned the SK channel family using methodology similar to that discussed above. Fragments of SK clones were first discovered when a virtual homology screen of an online expressed sequence tag database (ESTs, randomly cloned and sequenced cDNA fragments) identified a novel K⁺ channel pore-like region. This partial sequence was used, in a set of traditional library screens, to isolate and characterize three full-length cDNA clones²⁰. A fourth member of the mammalian family, an intermediate conductance, Ca²⁺-activated K⁺ channel, IK1, was later isolated²¹.

The human, mouse, and *Drosophila* genomes are fully sequenced. All genes with homology to known potassium channels have been identified, annotated, and classified. A description of current potassium channel classification follows. The discussion will focus on the three major groups of potassium channels emphasizing structural and functional similarities. This introduction will then conclude with a detailed treatment of SK channels.

Potassium Channel Phylogeny

The potassium channel super-family is the largest and most diverse of all ion channel families with 71 known loci in the mammalian genome²². Most

members of this super-family conduct potassium ions at rates approaching 10^8 ions per second, favoring potassium over sodium at a margin of 10^{413} . All members share the pore consensus sequence T/SxxTxGxG, with most members having the sequence TMxTVGYG²³. The super-family can be divided into three main structural family groups based on membrane topology: 4TM 2P (4 transmembrane, 2 pore), 2TM 1P, and 6TM 1P (Figure 1).

4 Transmembrane 2 Pore

Although the first member of this family was discovered in 1995²⁴, their existence was proposed as early as 1952 in the Hodgkin and Huxley model of the action potential 9. In their model the resting membrane potential is maintained around the potassium reversal potential by potassium “leak” channels. Amazingly Hodgkin and Huxley were correct. In 1996 it was shown that a member of this family from *Drosophila* was in fact voltage-independent and appeared to be always open with Goldman-Hodgkin-Katz rectification²⁵. However, not all members of this family are simply open pores, with family members regulated by diverse stimuli such as oxygen tension, pH, lipids, mechanical stretch, classic neurotransmitters, and G protein-coupled receptors²².

2 Transmembrane 1 Pore

In the presence of symmetrical potassium, most membrane preparations display high potassium conductance in response to depolarizing potentials and low conductance in response to hyperpolarizing potentials, a phenomenon called

Figure 1: Dendrogram of the 71 mammalian potassium channel alpha subunits. Branch length is proportional to evolutionary distance (ClustalW). The membrane topology of the three main subgroups is depicted.

Image duplicated from: Gutman, G.A., Chandy, K.G., Adelman, J.P., Aiyar, J., Bayliss, D.A., Clapham, D.E., Covarrubias, M., Desir, G.V., Furuichi, K., Ganetzky, B., *et al.* (2003). International Union of Pharmacology. XLI. Compendium of voltage-gated ion channels: potassium channels. *Pharmacol Rev* 55, 583-586.

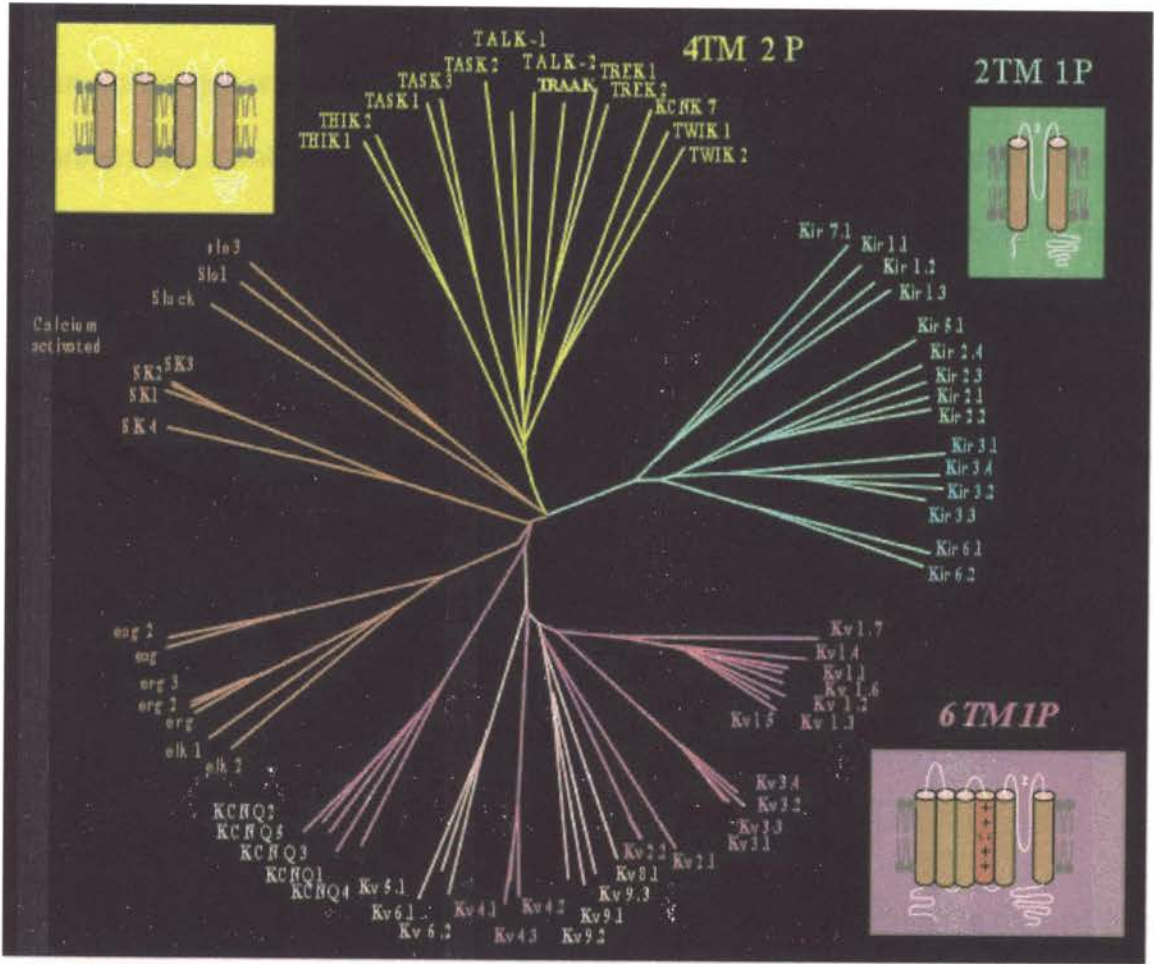


Figure 1.

outward rectification. In 1949 Bernard Katz first described atypical potassium channels with seemingly anomalous inward rectification, they were activated by hyperpolarization²⁶. Further investigation of other preparations showed that inward rectification is not as anomalous as it was first thought to be^{27; 28}. The first inward rectifier (Kir) cDNAs were cloned and expressed in 1993²⁹, and the mammalian genome now contains annotated loci for 15 known members²². Kir channels are involved in processes as diverse as the control of insulin release, heart rate, blood flow, and neuronal signaling²². Inward rectification is not a property of the channel itself, but is voltage-dependent block by intracellular Mg²⁺ and polyamines³⁰. The diverse list of substances that modulate Kir channels includes several intracellular factors, such as phosphatidylinositol 4,5-bisphosphate, arachidonic acid, Na⁺, Mg²⁺, pH, heterotrimeric G proteins, ATP, phosphorylation, redox potential, and interactions with PDZ (protein-protein interaction) domains³¹.

6 Transmembrane 1 Pore

This family is the largest and most diverse, and accordingly is divided into two functionally distinct subfamilies, voltage-gated and calcium-activated.

Voltage-gated 6TM 1P potassium channels include the classic delayed outward rectifier channels that open in response to membrane depolarization, repolarizing the membrane during the downstroke of the action potential as described in the Hodgkin and Huxley model. The fourth transmembrane segment (S4) of these channels is charged and acts as the voltage sensor³²⁻³⁴. Members

of this family are responsible for the M-current, behind long-QT syndrome (heart disorder), and were also the first family to be cloned from the original *Drosophila Shaker* mutant²². Voltage-regulated activation, inactivation, and deactivation of these channels affect action potential repolarization, duration, frequency, threshold and back-propagation. While all members of this subfamily are regulated by voltage, some members have coactivators (cGMP³⁵, Linoleic acid³⁶) or coinactivators (CamKII and calcineurin³⁷).

The calcium-activated 6TM 1P potassium channel subfamily contains eight members that can be divided into two distantly related groups based on sequence similarity (Figure 1).

The first group contains four members with relatively large conductance, between 60 and 260 pS³⁸. The most studied member of this large-conductance group is KCa1.1 (BK and *Slowpoke*). Under physiological conditions, this channel is activated in concert by calcium and voltage, and assists in membrane repolarization and afterhyperpolarization. Accordingly, this channel contains an S4 voltage sensor and there is evidence that calcium binds directly to the channel protein at three sites with differing affinity³⁹⁻⁴¹, although the site(s) of Ca²⁺ binding have not been unambiguously established. The other members of this group are not calcium-activated. Because of their clear homology they were included in this group when their amino acid sequences were first revealed, but before much functional characterization had been done. These remaining members are weakly voltage-activated and require pH, sodium, or chloride as

coactivators²². Members of this family are involved in membrane repolarization, hormone secretion, and muscle relaxation³⁸.

The final group of 6TM 1P calcium-activated potassium channels is the main focus of this dissertation. These channels have a relatively small unitary conductance of 9-11 pS and are completely voltage independent. The only known activator is Ca^{2+} , which binds to the beta subunit, calmodulin. The properties of the cloned SK channels will be discussed at length in a later section of this document.

Additional Diversity

The potassium channel superfamily is the largest of all ion channel families, and by extension, the most functionally diverse. The number of potassium channel genes, however, does not limit the range of functional diversity. Addition layers of functional diversity accumulate throughout the creation of a functional channel protein resulting in combinatorial complexity. After transcription, alternative splicing creates the first layer of intricacy, followed by post-translational modifications such as sumoylation, phosphorylation, ubiquitinylation, palmitoylation, and glycosylation⁴²⁻⁴⁴. During the assembly of a functional tetramer individual subunits can sometimes heteromultimerize with proteins coded by different genes within the subfamily⁴⁵⁻⁴⁷. Finally, some channels have associated accessory subunit proteins that modify channel function, but do not create functional channels on their own^{43; 48; 49}. The number

of possible combinations and permutations highlight the importance of potassium channels in fine-tuning excitability⁵⁰.

Structure

The key feature that designates a potassium channel is potassium selectivity. Indeed, the regions of highest homology among family members are the pore and selectivity filter. For some time scientists have known the membrane topology of the different potassium channel subfamilies, and that four (or two) subunits coassemble to form a functional pore⁵¹⁻⁵³, but high-resolution x-ray structures of the ubiquitous pore and selectivity filter were slow in coming due to the difficulties of crystallographic techniques applied to membrane proteins. Bacteria or cultured cells had been used in previous attempts to over express mammalian potassium channel protein for crystallization, but these efforts resulted in low quantities of insoluble protein. The laboratory of Rodderick Mackinnon came up with the simple and successful idea to over-express a bacterial potassium channel in bacteria. This technique has repeatedly produced sufficient quantities of protein for crystallization and several potassium channel structures^{13; 34; 54-56}. Many early theorists had suggested that the highly conserved pore sequence of potassium channel family members indicated underlying structural conservation. All of the current structures from the Mackinnon laboratory and others confirm this assumption with almost identical electron densities in the outer pore region and selectivity filter (Figure 2)⁵⁷. The structures, however, are more divergent at the inner pore, a region believed to be

Figure 2: Pore region, carbon backbone stereoviews of three crystallized potassium channels: Kv1.2 (red), KcsA (grey), and KvAP (blue). The highly specialized potassium pore displays a high level of structural conservation. **A**, Two opposite alpha subunits viewed from the side, through the plane of the membrane. **B**, Four alpha subunits viewed down the conduction pathway.

Image duplicated from: Long, S.B., Campbell, E.B., and Mackinnon, R. (2005). Crystal structure of a mammalian voltage-dependent Shaker family K⁺ channel. *Science* 309, 897-903.

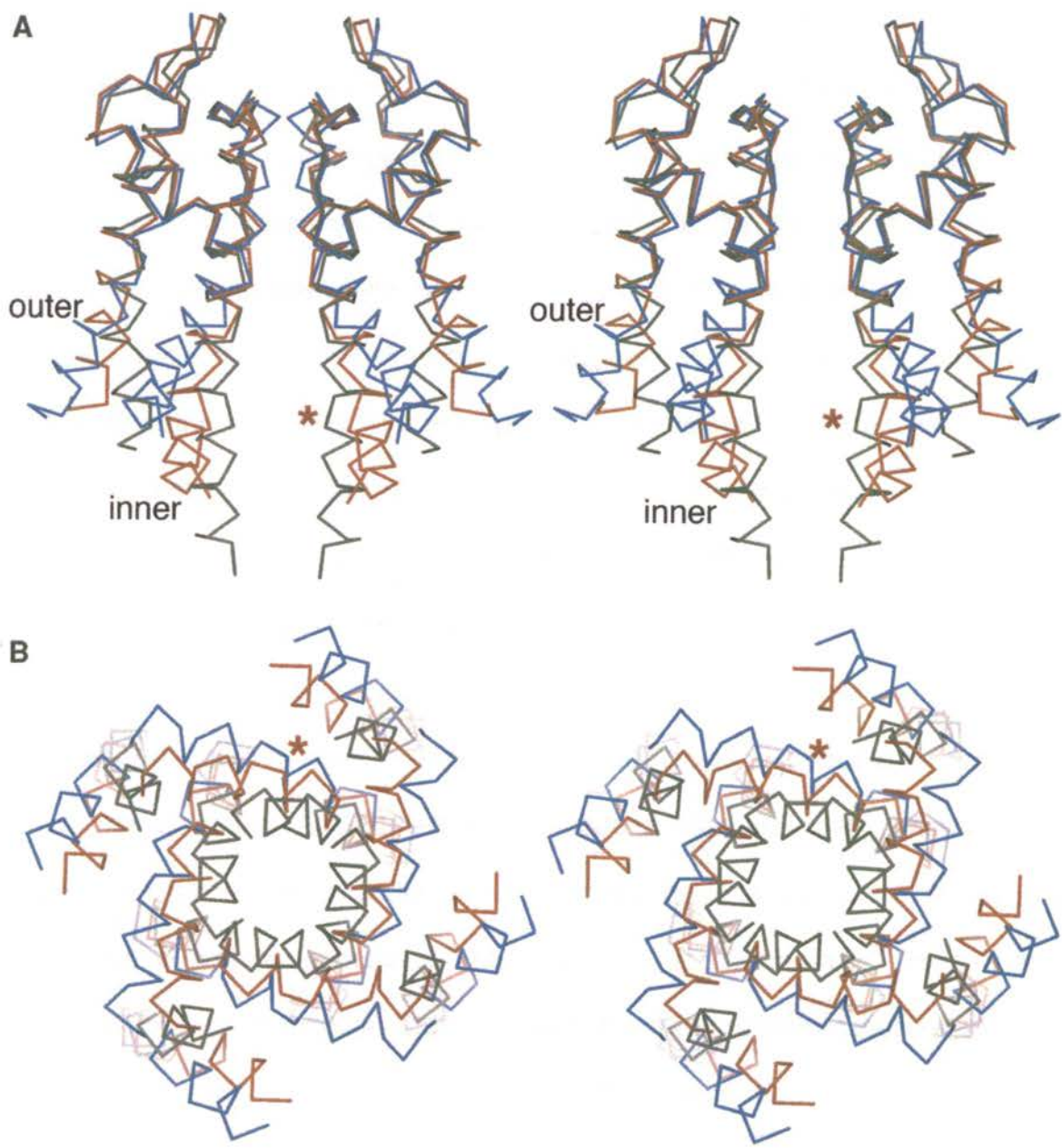


Figure 2

involved in gating. In general, regions of conserved function have identical structure. These structures have also greatly increased our knowledge of the apparently paradoxical properties of selectivity and high conduction velocity. Surprisingly the side chains of the GYG selectivity filter motif face away from the pore and backbone carbonyls face the lumen. This arrangement creates three stacked rings of carbonyls that substitute perfectly for the water molecules usually surrounding potassium ions in solution. In fact, there is almost no energy barrier associated with dehydration of a potassium ion. On the other hand, the carbonyls in the selectivity filter are spaced too far apart to compensate for the energetic cost of dehydrating a sodium ion. In this way potassium channels achieve conduction velocities approaching aqueous diffusion, while excluding sodium ions. The pore and selectivity filter are the only regions that all members of the potassium channel family have in common. As discussed above family members are gated by diverse stimuli, and the structures responsible for sensing these stimuli reflect that diversity⁵⁸⁻⁶⁰. Current structural data shows that potassium channels are modular, with the conduction pore and ligand binding or voltage-sensing regions encompassing separate structural domains⁶¹. How these separate domains fit together and the exact structural transitions between them remains unknown. Several papers report that these transition regions are frequently unstructured within the crystal lattice⁶². The calcium-sensing region of SK channels has been crystallized and its structure will be discussed at length later in this document.

Mammalian SK Channels

The small conductance calcium-activated potassium channel (SK) subfamily contains members SK1, SK2, SK3, and SK4 (IK) belonging to the 6TM 1P potassium channel family. Members of this family had been observed since 1958, but got their current name SK, in 1986 from the work of Blatz and Magleby⁶³. SK members SK1-3 were cloned in 1996 by the Adelman laboratory²⁰, and IK1 was cloned in 1997^{21; 64}. In 1998 calmodulin was identified as the beta subunit calcium sensor⁶⁵, and a crystal structure shortly followed⁶².

The Genes, Transcript Structure, and Cloned Channel Properties

SK channels, like voltage activated potassium channels, have six transmembrane segments, a reentrant pore loop, and charged residues in the fourth transmembrane segment, suggesting that SK channels evolved from voltage-activated potassium channels. The fourth transmembrane voltage sensor, however, is vestigial as SK channels are completely voltage independent. The highly conserved central core of the SK transcript contains six transmembrane domains, the pore, and the calmodulin-binding domain. This core region contains 6 to 7 intron-exon splice junctions that are conserved across the phyla suggesting a single ancestral gene. Transcripts consisting of just this core region form functional calcium-activated channels when expressed in heterologous systems, and are sufficient for most basic studies. As a result limited functional information is known about the intracellular termini (that extend beyond this core region) where the majority of transcript heterogeneity exists.

These termini contain many more exons with rather large introns, presumably containing regulatory sequences.

Heterologously expressed cloned SK channels are voltage independent; an increase in ambient calcium is the only thing that has been shown to activate these channels²⁰. When levels reach a few hundred nanomolar ($K_{0.5}$ of 330 nM for SK2⁶⁵), calcium binds to the SK beta subunit, calmodulin (CaM), activating the channel within milliseconds^{62; 65; 66}. Each SK transcript codes for one alpha subunit that crosses the membrane six times. Four SK alpha subunits coassemble with four CaMs to form a highly potassium-selective channel. These channels have a small unitary conductance of about ten picosiemens⁶⁷. All of the cloned SK channels are blocked by apamin, d-tubocurarine, and bicuculline, with unique EC50 values for the three mammalian clones⁶⁸⁻⁷⁰. The three human clones function in heterologous systems, but both rodent SK1 clones do not reach the cell surface (Figure 11) and have only been recorded as chimeras with other SK clones⁷¹.

Calmodulin, the Calcium Sensor

Early work in *Paramecium* provided the first evidence that calmodulin was the calcium sensor for various ion channels⁷². The *Pantophobiac* mutants overreact and *fast-2* mutants underreact to a noxious stimulus. Elegant work showed that *Pantophobiacs* lack a Ca^{2+} -activated potassium conductance and *fast-2* mutants lack a Ca^{2+} -activated sodium conductance, but the underlying genetic lesions are not in channel genes. Rather the mutations are single amino

acid changes in the E-F hands of calmodulin (CaM)⁷³⁻⁷⁶. Before CaM was identified as the calcium sensor for SK channels several key observations suggested the association. The calcium binding constants of CaM closely matches the submicromolar EC50 of calcium activation for SK. Furthermore, CaM is expressed in every cell type including those used for heterologous studies. Despite the volume of suggestive evidence, early experiments using well-known CaM inhibitors on expressed SK channels failed to establish a link between SK and CaM, potentially indicating another method of calcium sensing or a novel interaction with CaM. The breakthrough experiment that clearly showed functional coupling consisted of co-expressing SK along with mutated CaM⁶⁵. This special CaM had point mutations in the EF hand regions that reduced the affinity for calcium. SK currents recorded from these cells had reduced calcium sensitivity. Specifically, normal EF hands in the amino terminus were required for proper SK function while those in the carboxy terminus were not⁶⁶. Eventually crystals of the calmodulin binding domain (CaMBD) in complex with Ca²⁺/CaM were obtained, and the structure was solved (Figure 3)⁶². The structure confirmed that CaM is indeed in a unique association with the CaMBD. The dumbbell shaped CaM has four EF hand motifs that usually bind a total of four calcium ions. Two lobes, N- and C-terminal, are separated by a flexible linker with two EF hands per lobe. In the structure with the CaMBD the C-terminal lobe of CaM does not bind calcium, but instead provides the anchoring point for the constitutive association with the channel alpha subunit. Two calcium ions are resolved in the crystal structure, and coordinated by the two EF hands in

Figure 3: **a**, Ribbon diagram of the CaMBD/Ca²⁺/CaM dimeric complex. CaMBD subunits are in blue and yellow, CaM molecules are in green, and the Ca²⁺ ions are in red. Secondary structural elements, the CaM linker and the first and last observed residues in the CaMBD are labeled. **b**, View in **a** rotated by 90° showing the orientation of the complex relative to the membrane. Arrow indicates the positions of the first observed residue of each of the CaMBD monomers that are linked to the S6 pore helices. Figure generated with MOLSCRIPT.

Figure and legend duplicated from: Schumacher, M.A., Rivard, A.F., Bachinger, H.P., and Adelman, J.P. (2001). Structure of the gating domain of a Ca²⁺-activated K⁺ channel complexed with Ca²⁺/calmodulin. *Nature* 410, 1120-1124.

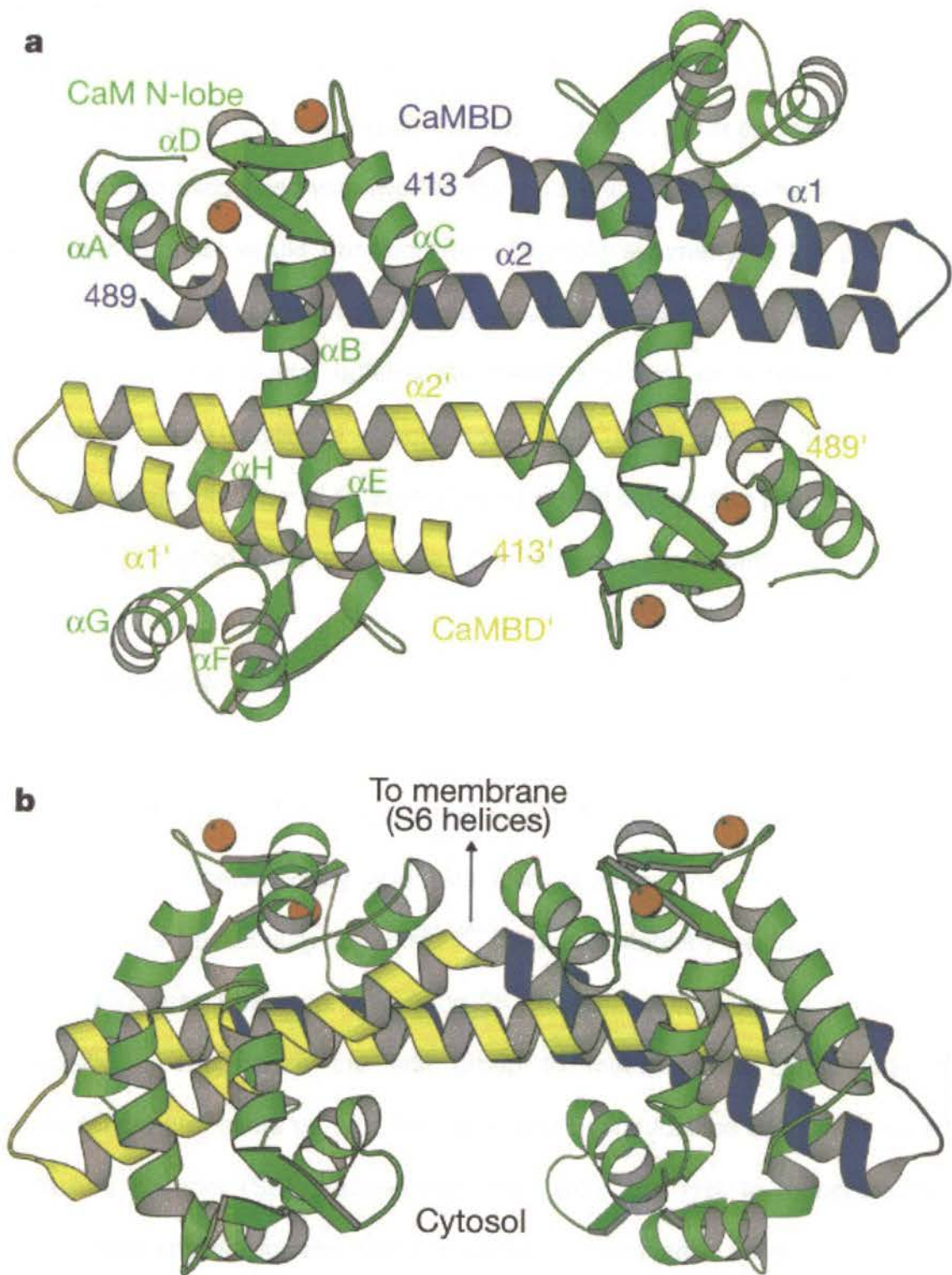


Figure 3.

the N-terminal lobe. The structural data agrees perfectly with the previously discussed functional mutagenesis studies. Another interesting aspect of the structure is that it does not display four-fold symmetry. Instead two calmodulin molecules are associated with two SK alpha subunits, meaning that a functional tetrameric channel would transition from four-fold symmetry at the pore to a dimer-of-dimers just beneath the membrane. It is not clear if the structural data obtained from the crystal reflects the native structure of a tetramer in the membrane⁶¹. The published structure was of a small domain from a large channel protein, and should be treated as such until further data support or refute it. Indeed, published⁷⁷ and unpublished data conflict in this regard.

In Vivo Studies

Early studies observed calcium-activated potassium currents in erythrocytes¹⁴, aplysia⁷⁸, cat spinal neurons⁷⁹, hippocampal neurons⁸⁰⁻⁸², and hepatocytes⁸³. Contemporary scientists also observed that the peptide toxin apamin blocked potassium currents^{84; 85}. Blatz and Magleby performed some of the most extensive pioneering work on SK channels using cultured rat skeletal muscle^{63; 86}. They were the first group to measure the single channel conductance, and came up with the name small conductance calcium-activated potassium channel (SK). Furthermore, they were the first to recognize that apamin was specific for this class of potassium channels. Later work on SK channels in skeletal muscle showed that their expression is aberrant in adult

muscle, only occurring before innervation, after mature muscle denervation, or in diseased (myotonic muscular dystrophy) muscle⁸⁷⁻⁹⁰.

The group of Michel Lazdunski has been a leader in the SK field, and were among the first to work with apamin, even developing a method of incorporating ¹²⁵I into apamin. Radioactive apamin could be used as a histological stain⁹¹, eventually found to be specific for SK channels. In 1982 the Lazdunski group realized that apamin blocked a class of calcium-activated potassium channels^{92; 93}. A year later they suggested that apamin might be specific for SK channels and have little or no additional pharmacology⁹⁴. The specificity of the toxin is now largely accepted, with many scientists referring to apamin-sensitive current as SK current. As a result most recent *in vivo* SK studies rely solely on the specific pharmacology of apamin.

In addition to the early apamin binding studies other traditional methods have been used to localize SK channels. When SK channels were cloned, *in situ* hybridized rat brain sections revealed that SK1, 2, and 3 have distinct but overlapping expression patterns²⁰. The highest levels of expression were seen in the hippocampus, pontine nucleus, thalamus, cerebellum, olfactory bulb, and cortex. Subsequent antibody staining of rodent brains produced similar results⁹⁵. In addition to the central nervous system SK1, 2, and 3 are found in organs such as the liver, heart, lung, prostate, pancreas, colon, and kidney³⁸. SK4 (IK) appears to be limited to the periphery with highest concentrations in blood and epithelial cells³⁸.

Open potassium channels shift the membrane potential toward the potassium reversal potential. This effect counters excitatory sodium and calcium currents and returns membrane potentials to resting levels. During excitation most neurons experience a transient increase in calcium concentration. If present, SK channels open in response to the increased calcium concentration and dampen excitation creating negative feedback. After an action potential, SK channels can contribute to a current that hyperpolarizes a cell, making the membrane potential more negative than it is at rest. This afterhyperpolarization (AHP) can create feedback so strong that it prevents a cell from firing. SK current duration directly reports calcium levels and persists until intracellular calcium is buffered or sequestered.

In mammals, SK channels serve a variety of roles. In many central neurons, SK channels regulate firing frequency by contributing to the afterhyperpolarization that follows an action potential^{96; 97}. In CA1 hippocampal neurons SK channels influence synaptic plasticity by modulating NMDA receptors⁹⁸, and shape dendritic Ca^{2+} transients that may modulate dendritic integration⁹⁹. In peripheral tissues, SK channels regulate hormone release¹⁰⁰⁻¹⁰³ and regulate smooth muscle tone¹⁰⁴⁻¹⁰⁶. Recently knockout mice for all of the SK genes have been generated^{107; 108}. SK2, 3, and 4 mice display overt phenotypes, but SK1 mice appear to be aphenotypic. SK2 channels were confirmed as those responsible for afterhyperpolarizing currents in hippocampal CA1 neurons. SK3 channels affect respiration and parturition of mice¹⁰⁹. SK1 null mice remain a

mystery, furthermore, no *in vivo* currents have been convincingly attributed to SK1 and clones do not function in heterologous systems.

***Drosophila* SK**

Drosophila has served as a model organism for investigating the roles of many different ion channels^{110; 111}. The short generation time and the ease with which genetics and biochemistry can be combined with behavioral and electrophysiological assays have provided insights and directions that have shaped studies of mammalian orthologues. For K⁺ channels, the larval muscle preparation has not only served to investigate biophysical and physiological aspects of several different channel types, it also was instrumental in the isolation of the first K⁺ channel clones, the *Shaker* voltage-dependent channel¹⁶. Early studies on the other major subtypes of voltage-gated K⁺ channels (*Shab*, *Shal*, and *Shaw*), and the Ca²⁺- and voltage-gated BK channel encoded by the *Slowpoke* gene also took advantage of the larval muscle preparation¹¹²⁻¹¹⁴. The *Drosophila* coding sequences were used as probes to identify the corresponding mammalian genes. In all of these cases, there was a clear correspondence between channel activity recorded and characterized in *Drosophila* and K⁺ channel activity in mammalian organisms, and these activities were generally recapitulated by heterologous expression of the cloned *Drosophila* and mammalian channels¹¹⁵⁻¹¹⁸. In contrast to the other major classes of K⁺ channels, there are no clear demonstrations of SK channel activity from *Drosophila*.

There are four potassium conductances that have been characterized in *Drosophila* larval muscle. I_A and I_K are voltage activated and I_{CF} and I_{CS} are calcium activated¹¹⁹. The channel genes responsible for these potassium conductances have been identified, all except for the I_{CS} channel. Many have assumed that *Drosophila* SK (dSK) is responsible for the calcium-activated potassium conductance, the I_{CS} . Therefore, to investigate the cellular and physiological roles of SK channels and to take advantage of the unique opportunities offered by *Drosophila*, we decided to generate an SK null mutant and investigate the role *Drosophila* SK channels.

Chapter II. Methods

dSK Gene Characterization. Probes representing highly conserved regions of mammalian SK channels were used in two screens, one of a *D. melanogaster* head cDNA library and a second virtual screen of the published *D. melanogaster* genome¹²⁰. Sequences obtained from the cDNA library were extended in the 5' and 3' direction using standard RACE (rapid amplification of cDNA ends) protocols. Bloomington stock number P12729 (FlyBase ID FBst0012729) contains a P{GT1} insertion at position 41166 of release 3 scaffold AE003434¹²⁰; ¹²¹. The insertion resides in the center of what is likely the first SK intron. These flies were used for gamma irradiation to 'hop' the P-element.

Northern Blot. Live adult flies (100) were frozen and ground to a fine powder under liquid nitrogen. RNA was extracted from the cold powder using 500 µl of chilled Sigma Tri-Reagent according to the manufacturers protocol. RNA was resuspended in 50 mM MOPS, 12.5 mM Na Acetate, 2.5mM EDTA, all at pH 7.0, together with 15% formamide and 2% formaldehyde. RNA (from about 50 flies) was denatured at 65 °C for 10 min. and then separated (80 mV) through a 1.4%/6% agarose/formaldehyde gel (80 mV) containing 20 mM MOPS, 5 mM Na Acetate, 1 mM EDTA, (pH 7.0). Following separation the RNA was capillary-blotted onto Magnacharge membrane (Osmonics) in 20X SSC, and UV crosslinked to the membrane with a Stratalinker (Stratagene). The membrane was prehybridized for two hours at 65°C in 400 mM NaPO₄, 1 mM EDTA, 5%

SDS and, 50% formamide. BSA and salmon sperm DNA were both added at 1 mg/ml to decrease background. From linearized templates cloned into pBluescript (Stratagene), ribo-probes were transcribed with T7 polymerase (Stratagene) according to the manufacturers protocol with the addition of α -³²P-UTP (Perkin Elmer). Reactions were treated with DNase (Ambion) and then purified over a Centri-Spin 10 column according to the manufacturers protocol (Princeton Separations). Probes were denatured at 70°C for 10 minutes, added to hybridization solution, and incubated with the blots at 65°C for 12 hours. Blots were washed several times at 75°C with a solution containing 0.1% SSC, 0.1% SDS, and 1.0 mM EDTA. Radioactive signals were detected using Phosphorimager 445 SI (Molecular Dynamics, Sunnyvale, CA).

Quantitative PCR Flies were raised and maintained at 25°C. Staged larvae and embryos were collected on standard fruit juice agar plates¹²². For collection of heads and bodies, fattened adults were first frozen in liquid nitrogen and then vortexed in a 50 ml Falcon tube. Adult heads were then separated from bodies using sieves (US series sizes 25 and 45). RNA was purified from 45 mg of tissue using Sigma Tri-Reagent according to the manufacturers protocol. RNA was resuspended in nuclease-free water to a final concentration of 1.5 μ g/ μ l. Complimentary DNAs were synthesized from 4.5 μ g of purified RNA using random hexamers and murine Moloney leukemia virus reverse transcriptase according to the manufacturers protocol (Gibco). Quantitative PCR was performed on an Opticon OP346 (MJ Research) for 50 cycles at 94 °C for 15 s

and 71°C for 40 s. Primers were designed using MIT's PRIMER3 software 123 as described¹²⁴: dSK GCGTCAGTGCGAAAGGTTCC and CGCCGTAGCCGACACACAG, dActin TGCAGCGGATAACTAGAACTACTC and CAAAGGAGCCTCAGTAAGCAAG. PCRs (20 µl) contained 2 µl of 10X PCR buffer, 2.5 mM MgCl₂, 200 µM dNTPs (Roche), 0.25 µM primer, 1X SYBR green (Invitrogen), and 1 unit of Platinum Taq (Invitrogen). Reactions were separated on 3% agarose gels to verify the presence of a single amplicon and the absence of primer dimers.

Drosophila SK RNA levels were calculated with the relative standard curve method as described in User Bulletin #2¹²⁵, using serially diluted adult male cDNA (the efficiency of the reverse transcription reaction was similar between RNA samples) to construct the standard curve. Levels of SK RNA were normalized to the levels of Actin RNA (another SK amplicon along with RP49 as a normalizer produced similar results, data not shown). The experiment was performed three times and standard deviations were calculated as described in User Bulletin #2¹²⁵.

Electrophysiology. Chinese Hamster Ovary (CHO) cells were grown in F-12 Nutrient Mixture supplemented with 10% heat-inactivated fetal bovine serum and penicillin-streptomycin (Invitrogen, Carlsbad, CA). Cells were transfected with the CMV-based expression plasmids pJPA encoding the indicated channel and pEGFP (Clontech, Mountain View, CA) encoding GFP for identification of

transfected cells. Transfections were performed with Lipofectamine 2000 according to the manufacturer's protocol (Invitrogen, Carlsbad, CA) using channel and GFP plasmids in a ratio of 20 to 1. Whole-cell recordings were performed at room temperature 12-48 hours post transfection. Electrodes pulled from thin-walled borosilicate glass (World Precision Instruments, Sarasota, FL) had tip resistances of 3-5 M Ω . Voltage-clamp recordings were performed with an EPC9 amplifier (HEKA, Lambrecht, Germany). Pipettes were filled with (in mM) 140 KCl, 10 HEPES, and 0.2 CaCl₂ or 5 EGTA adjusted to pH 7.2. The bath solution contained 30 KCl, 110 NaCl, 10 HEPES, 1 MgCl₂, and 1CaCl₂ adjusted to pH 7.2. TEA was dissolved in bath solution and adjusted to pH 7.2. In the whole-cell configuration 2-second voltage ramps from -80 mV to +80 mV were used to elicit currents. Only current responses with reversal potentials within \pm 5 mV of the predicted K⁺ reversal potential (-38 mV) were used for analysis.

Electrophysiology (Larval Muscle Preparation). The *Drosophila* third instar larvae fillet was prepared as previously described¹²⁶. Larvae were dissected in ice-cold Ca²⁺-free Ringer's solution and body wall muscles 6 and 7 were recorded from in the two-electrode, voltage-clamp configuration. Electrodes filled with 3 M KCl had tip resistances of 5-7 megaohms. Larvae were bathed at 4° C in the following Ca²⁺-free recording solution (in mM): 128 NaCl, 2 KCl, 20 MgCl₂, 75.5 Sucrose, 5 HEPES, and 0.5 EGTA. Cells were clamped at -80 mV prior to voltage ramp commands from -110 to -40. After the first ramp the bath solution was exchanged with one containing Ca²⁺ (4 mM MgCl₂, and 20 mM CaCl₂)

Immunocytochemistry. was performed as previously described 77, COS-7 cells were grown to ~15% confluency in a 60-mm dish on microscope cover glasses and incubated for 5 h with the transfection mixture of 2.75 µg of DNA (ratio of GFP:SK2:CaM, 1:5:5) in 1 ml of DMEM and 8 µl of DMRIE-C reagent (Invitrogen) in another 1 ml of DMEM. The mixture was incubated at room temperature for 20 min. prior to cell treatment. After transfection, cells were washed and fed with complete medium and incubated at 37°C in 5% CO₂. Immunocytochemistry was performed 1–2 days post-transfection. Live cell staining was performed by incubating the cells at 37°C with 1:250 dilution of anti-myc monoclonal antibody (Invitrogen) in complete medium for 1 h. After three washes in complete medium and two washes in PBS⁺ (1x phosphate-buffered saline containing 1 mM MgCl₂ and 0.1 mM CaCl₂), cells were fixed with 4% formaldehyde at room temperature for 15 min. After quenching with two washes of 50 mM NH₄Cl in PBS⁺, cells were washed once with PBS⁺. Nonspecific binding was then blocked by incubating the cells with 10% bovine serum albumin (BSA) in PBS⁺ at room temperature for 30 min. The excess BSA was removed and the secondary antibody (1:500 dilution of Texas Red-conjugated horse anti-mouse IgG (H+L), Vector, Burlingame, CA) was applied at 4°C overnight. Cells were then washed three times with PBS⁺ and mounted (ProLong Antifade Kit, Molecular Probes, Eugene, OR) for imaging.

For permeabilized labeling, cells were washed with PBS⁺ and fixed with 4% formaldehyde at 4 °C for 30 min. After washing three times with ice-cold PBS⁺, cells were permeabilized with 0.2% Triton X-100 in PBS⁺ at room

temperature for 15 min. To remove excess Triton X-100, cells were washed five times with PBS⁺ at room temperature. Nonspecific binding was then blocked by incubating the cells with 10% BSA in PBS⁺ at room temperature for 30 minutes. Primary antibody was then added and incubated at 4°C overnight. The next day, the cells were washed and incubated with the secondary antibody at room temperature for 1 h. Cells were washed again, and mounting was performed as described for non-permeabilized cells. Images were acquired with epifluorescence using an optical microscope (Axioplan2, Zeiss, Thornwood, NY) and the program OpenLab (Improvision, Lexington, MA)

Chapter III. Results

Summary

The *Drosophila* genome contains a single gene that encodes a small conductance Ca^{2+} -activated K^+ channel (SK channel; dSK). The intron-exon mosaic of the dSK gene revealed several alternative N-terminal splice products as well as two exons that comprise precise pore loop (P-loop) alternatives. Northern blot and quantitative PCR analyses showed that there are two dSK transcripts that are developmentally regulated, with the highest levels of expression found in adult head. *Drosophila* SK null flies generated by gamma ray deletion had no overt behavioral phenotype. Heterologous expression of dSK cDNA in either *Drosophila* or mammalian cell lines showed that the expressed protein fails to reach the plasma membrane. Chimeric channels containing the intracellular N- and C-terminal domains of mouse SK2 do reach the plasma membrane and the expressed channels do not require Ca^{2+} for gating, are sensitive to the generic K^+ channel blocker TEA (tetraethylammonium), and insensitive to the SK channel specific blocker apamin. These results suggest that the dSK channels may reside on intracellular organelles, or may require an unidentified auxiliary subunit for plasma membrane expression.

dSK Gene Characterization

A virtual screen of the *D. melanogaster* genome using mammalian SK channel sequences identified a single dSK gene. Exons encoding

transmembrane segments 1-6 (S1-6) and the CaMBD were readily identified because of their conserved amino acid sequence with mammalian SK channels. For this core region of the channel (S1-6, pore A, and, CaMBD) dSK had pairwise alignment scores of 69, 71, 70, and 40 when aligned with mouse SK1, 2, 3, and 4 (respectively) using the CLUSTALW algorithm¹²⁷. Interestingly the dSK gene contained two pore exons, one with a 'GYG' selectivity filter and one with a 'GFG' selectivity filter (fig 4c). Correspondingly, a traditional screen of adult head cDNAs identified two dSK coding sequences with the two different pores.

The cDNAs were extended in the 5' and 3' direction using rapid amplification of cDNA ends (RACE) protocols. Splice variants were detected at both termini. At the 5' end, splice variants resulted in transcripts that had one of two large 5' untranslated regions (UTR), one UTR preceding exon 1 and the other UTR preceding exon 2 (see Appendix Figure B). The other 5' splice variants were small changes within the two large transcripts. At the 3' end transcripts were identified that ended the open reading frame at exon 12 or at exon 13, with similar 3' untranslated regions for both (see Appendix Item D). The longest dSK transcript, exons 1-13 (Figure 4a), was compared to the full-length mouse SK protein sequences. Pairwise alignment scores were 53, 52, 45, and 39 for mSK1, 2, 3, and 4 respectively¹²⁷. These scores compared with those for the S1-6 and the CaMBD highlight the conservation of the core region and divergence of the N- and C-termini across the phyla (Figure 4a).

In addition to the two UTR regions identified by RACE PCR (discussed

Figure 4: *Drosophila* SK sequence comparison. **A**, Amino acid alignment of dSK with the four murine SK clones generated with the ClustalW algorithm (default conditions on embl website) 4. **B**, Phylogenetic tree of aligned sequences ¹²⁷. **C**, Alignment of the two alternate pore exons (7a and 7b) ¹²⁷. Figure panels **A** and **B** were made with the online program BoxShade written by Kay Hofmann and Michael D. Baron.

A

```

mSK2 1 YALIFGMFGIVVMVIETELS-WGAVDKASLYSLALKCLISLSTVILLGLIIVYHAREIQOL
mSK3 1 YALIFGMFGIVVMVIETELS-WGLYSKDSMPSLALKCLISLSTVILLGLIIAYHTREVQL
mSK1 1 YALIFGMFGIVVMVIETELS-WGVYTRKESLCSFALKCLISLSTVILLGLVILYHAREIQOL
dSK 1 YALVMGMFGIIVMVIENELSSAGVYTRKASFYSTALKTLISVSTVILLGLIVAYHAEVQL
mSK4 1 WALVLAGTGI GLMVLHAEML-WFLGCKWVLYLLLVKCLITLSTAFLLCLIVVFHAKVQL

mSK2 60 FMVDNGADDWRIAMTYERIFFICLELVCAIHPVPGNYTFWTARLAFS-YAPSTTTADV
mSK3 60 FVIDNGADDWRIAMTYERIFYISLEMLVCAIHPVPGYKFFWTARLAFS-YTPSRAEADV
mSK1 60 FLVDNGADDWRIAMTWERVSLISLELVCAIHPVPGHYRFTWTARLAFS-LVPSAAEADL
dSK 61 FMIDNCADDWRIAMTQRISQIGLELFCVCAIHPVPGVYFQWTKLANKNKTIGTEMVPPY
mSK4 60 FMTDNGLRDWRVALTRRQVAQILLELLVCGVHPVPLRSPHCALAGEATDAQPWPFGFLGEG

mSK2 119 DIILSIPMFLRLYLIA RVMLLHSLKFTDASSRSIGALNRKINFNTRFVMKTLMTICPGTVL
mSK3 119 DIILSIPMFLRLYLIA RVMLLHSLKFTDASSRSIGALNRKINFNTRFVMKTLMTICPGTVL
mSK1 119 DVLLSIPMFLRLYLIA RVMLLHSRIIFTDASSRSIGALNRVINFNTRFVTKLMTICPGTVL
dSK 121 DVALSEIPMFLRLYLICRVMLLHSLKFTDASSRSIGALNRKINFNTRFVTKLMTICPGTVL
mSK4 120 EALLSLAMLLRLYLVPRAVLLRS GVLLNASVRSIEALNQVRFHWFVAKLYMNTHPGREL

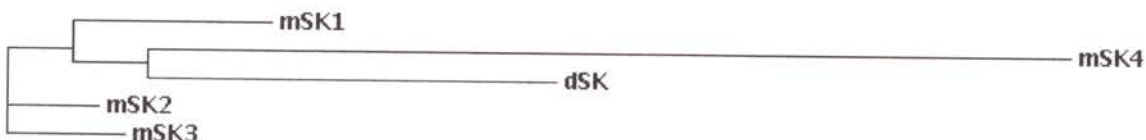
mSK2 179 LVFSISLWIIAAWTVRA CERYHDQODVTSNFLGAMWLISITFLSIGYGDMPNTYCGKGV
mSK3 179 LVFSISLWIIAAWTVRVCERYHDQODVTSNFLGAMWLISITFLSIGYGDMPHTYCGKGV
mSK1 179 LVFSVSSWIIAAWTVRVCERYHDQODVTSNFLGAMWLISITFLSIGYGDMPHTYCGKGV
dSK 181 LVFMVSLWIIASWTLRQCERFHD--EEHANLLNSMWLTAITFLCVGYGDVVPNTYCGRGI
mSK4 180 LGLTGLWLTTAWVLSVAERQAVN--ATGHLTDTLWLLPITFLTIGYGDVVPGTMWGKIV

mSK2 239 CLLTGIMGAGCTALVVAVVARKLELTKAEKHVHNFMMDTQLTKRVKNAANVLRWLIY
mSK3 239 CLLTGIMGAGCTALVVAVVARKLELTKAEKHVHNFMMDTQLTKRVKNAANVLRWLVY
mSK1 239 CLLTGIMGAGCTALVVAVVARKLELTKAEKHVHNFMMDTQLTKRVKNAANVLRWLIY
dSK 239 TLTCGMVGAGCTALVVAVVSRKLELTAEKHVHNFMMDTQLTKRVKNAANVLRWLIY
mSK4 238 CLCTGMVGVCTALVVAVVARKLEFNKAEKHVHNFMMDIHYAKEMKESAAARLQSAWVY

mSK2 299 KNTKLVKKIDHAKVRKHQRKFLOAIHQ---LRSVKMEQRKLNDOANTLVDLAKTONI
mSK3 299 KHTKLVKKIDHAKVRKHQRKFLOAIHQ---LRGVKMEQRKLSDOANTLVDLAKMONV
mSK1 299 KHTRLVKKPDQGRVRKHQRKFLOAIHQAKLRSVKIEQGVNDQANTLAEAKAQSI
dSK 299 KHTRLVQRVNPGRVTRHQRKFLAIYA---LRKVKMDQRKLMNANTLTDMAKTONT
mSK4 298 KHTR---RKDSRAARRHQRKMLAAIHT---FRQVRLKHKRLREQVNSMVDISKMHMT

```

B



C

```

7a 1 FHDEEHANLLNSMWLTAITFLCVGYGDIVPNTYCGRGI TLTCGMV
7b 1 FHDEEHANLLNAMWLI AITFLSVGFGDIVPNTYCGRGI AVSTGIM

```

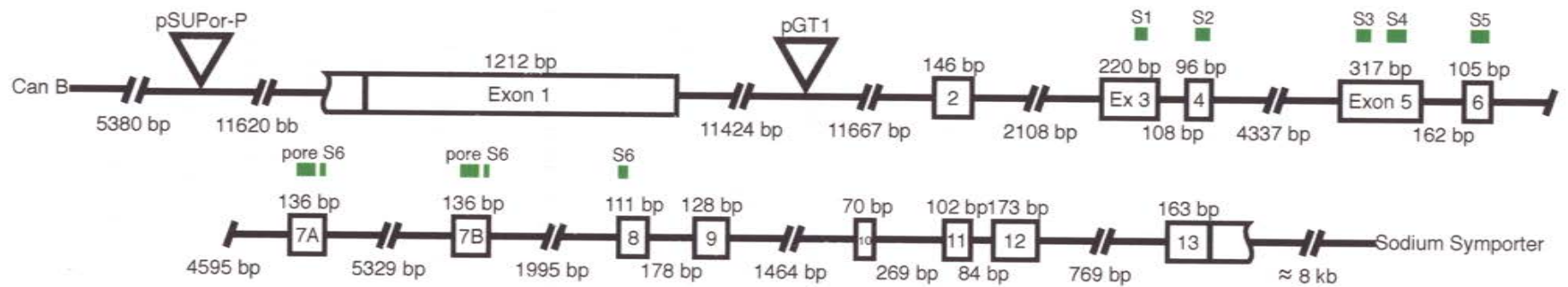
Figure 4

above), two transcription start sites are annotated (Flybase) at the 5' end of each UTR. The two separate UTRs and transcription start sites suggest that there are two transcripts with separate promoters (see Appendix Figure B). Flybase annotation also indicates P-element insertions clustered immediately adjacent to the predicted transcription start sites. The presence of these two clusters of insertions further strengthens the two-promoter hypothesis because P-elements tend to land near promoters¹²⁸. In order to test this hypothesis two P-elements (Bloomington stock numbers P13102 and P12729 shown in Figure 5) were mobilized with the Delta 2-3 transposase (standard mobilization cross). Diagnostic RT-PCR primers were designed that specifically amplified each of the two transcripts. Successful imprecise excision of the P13102 (pSUPor-P) element specifically eliminated the long dSK transcript that begins with exon 1. The exact genomic break points that resulted in elimination of the exon 1 containing transcript were not mapped, but genomic PCRs using primer pairs 4kb on either side of the P-element insertion site indicate that deletions need not be bigger than 8kb for specific exon 1 containing transcript ablation. The identical experiment was performed for the transcript that begins with exon 2, using the P12729 (pGT1) element, with identical results.

Both transcripts must contain vital promoter sequence within 4kb on either side of the P-element insertion sites. With this fact in mind the 8kb of genomic sequence centered on each P-element insertion site was amplified, subcloned into the pPTGAL vector¹²⁹, and sent to the Duke Model System Genomics Group for *Drosophila* transformation. Transformants containing the pPTGAL plasmid

Figure 5: Intron/exon mosaic of the SK gene on the X chromosome at cytological position 4F 2-8. Of note are the two pore exons (7a and 7b). The location of transposable elements as well as the flanking genes CanB and a putative sodium transporter are depicted. Transposable elements usually land near promoters. The annotated *Drosophila* genome also predicts two promoters at the location of the transposable elements (corresponding to the two transcripts seen on the Northern blot in Figure 8). Imprecise (approximately 6kb flanking DNA) transposase mediated excision of the two elements resulted in specific elimination of either transcript class (determined by PCR). SK nulls (3.2 and 7.2) lack approximately 44 kb of DNA covering exons 3-6.

Figure 5



with dSK promoter inserts are designed to express the yeast Gal4 protein under the specific dSK promoter. In yeast, the native Gal4 protein binds to the upstream activating sequence (UAS) initiating transcription of galactose operon genes following the UAS. *Drosophila* geneticists have adopted the yeast Gal4/UAS elements and created a modular, bipartite expression system¹³⁰. In this system putative promoter sequence can be used to drive Gal4 expression in a transgenic fly line. When this Gal4 line is crossed with a transgenic line with UAS driving GFP, Gal4 expressing cells become GFP expressing cells. Separating the Gal4 activator and the UAS reporter into separate driver/responder transgenic lines allows geneticists to mix and match promoter/reporter combinations with a simple cross. GFP expression was not detected in any of dSK driver line crosses. Progeny from crosses were observed with standard and confocal fluorescence microscopy. Furthermore, Gal4 antibodies failed to detect Gal4 protein in extracts of dSK driver flies prepared as Western blots. These results suggest that the promoter regions isolated contain very weak promoters, or that these regions are missing associated enhancers.

Transgenic lines were also generated (Duke MSG) with the pUAST¹³¹ plasmid. These responder lines were designed to express dSK and dSK with a triple myc tag (see Appendix Item E) under UAS control. Both lines were successfully generated as determined by genomic PCR confirmation of integration. Attempts were made to drive the dSK responder lines with the actin promoter¹³² and the neuronal *elav*¹³³ promoter. None of the crosses resulted in progeny with an overt phenotype. Furthermore, dSK protein could not be

detected with myc or custom monoclonal dSK antibodies (antibodies discussed below). These results agree with failed attempts to express dSK in the *Drosophila* S2 cell line (discussed below). Finally, control crosses of actin/*elav* Gal4 driver lines with UAS GFP reporter lines confirmed that the system was functioning correctly.

Generation of dSK-null Flies

Several attempts were made to generate SK nulls. First, attempts were made to mobilize the transposable element P12729 using the transposase Delta 2-3. Second, a targeted approach as outlined by Kent Golic was initiated¹³⁴. Lastly attempts were made to mobilize P12729 using gamma rays. The transposase method was abandoned because the resulting deletions were consistently too small to affect both of the major transcripts (as assayed by RT-PCR and Northern blots). The targeted approach was abandoned because at the time it was a new method and had not been replicated by many that had attempted it. Fortunately the gamma ray deletion method proved successful and a description of it follows.

dSK null flies were generated by gamma ray deletion of P12729 males (Figure 6a). To be large enough to eliminate SK coding sequence but small enough that flanking genes were left intact, deletions needed to be between 12 and 60kb. Favorable mutations were identified in a three step screening process. First, the loss of the P-element dominant marker mini-white in the F1 progeny indicated a deletion in SK. Second, we screened for normal cytology of the SK chromosomal region (Figure 6b) as determined by polytene chromosome

Figure 6: **A**, mating scheme used for generation of gamma ray mediated SK nulls. **B** and **C**, Polytene chromosome squash. Proximal end of the polytene, X chromosome stained with orcin. **B**, Normal cytology, null mutant dSK3.2 showing intact banding at the dSK locus, 4F3-7. **C**, Abnormal cytology, the large deletion isolated spanning 4C15-5B8.

A

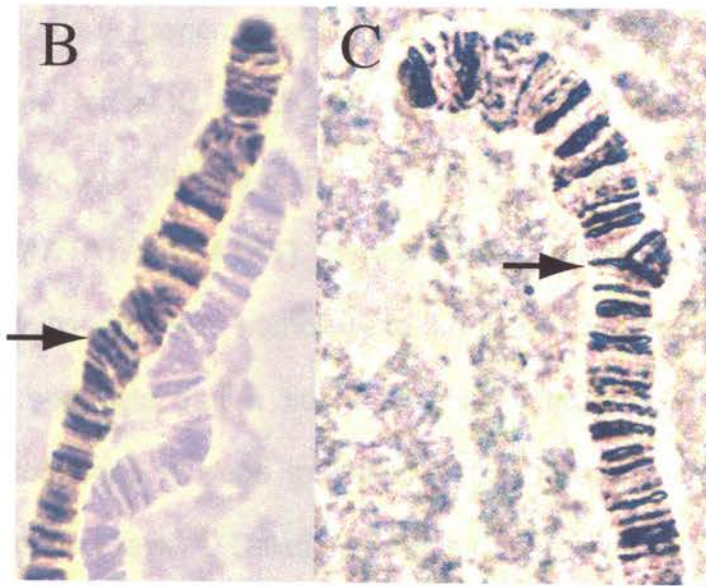
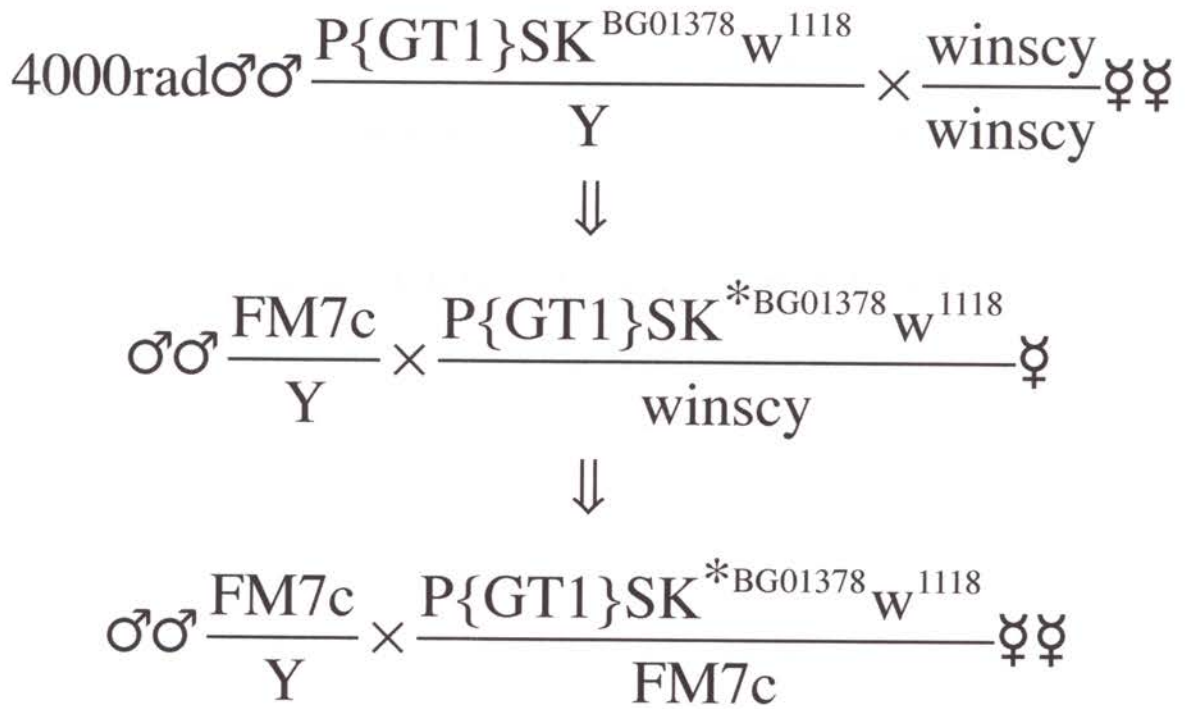


Figure 6

staining, indicating a deletion smaller than ~100kb (Figure 6c). Finally, mutants must lack dSK rtPCR products and have intact rtPCR products for flanking genes (Figure 7). Favorable deletions were approximately mapped with PCR on genomic DNA. Primers were designed for amplicons of about 300 base pairs that marched out in 2.5kb intervals from the P-element insertion point. Primer pairs that gave appropriate products for control wild-type flies but not for mutants were determined to be in deleted sequence. After rough mapping, the exact break points were determined by PCR amplification and DNA sequencing of the break point region.

The mutagenesis screen resulted in two independent ~44kb deletions (dSK3.2 and dSK7.2) that eliminated the coding sequences for transmembrane segments 1-5 and one of the alternative pores. Another isolate comprised a large deletion spanning polytene segments 4C15-5B8 (mapped by polytene chromosome squashes, see figure 6C). The 44kb deletions have identical 3' break points (unique genomic sequence on either side of the break point indicated by the letter X, CACAAACAGGCXGTATGAACCCA) and 5' break points that differ by 1.3kb (3.2, GGTGCATACCAXTAAATGAATTC, and 7.2, CTATACATACAXTATACATATAT). Between these break points, both deletions contain a 2.7kb insertion with homology to the *Hobo* transposase (see Appendix Item A). This suggests that a subpopulation of the original strain used for mutagenesis contained a *Hobo* insertion at this location and that *Hobo* was mobilized by gamma rays¹³⁵. Deletions of this nature with one identical and one variable break point have been previously reported for genomic rearrangements

Figure 7: Ethidium stained agarose gel of RT PCR products showing that two candidate nulls lack SK transcripts. RT PCR was performed on the parental P-element strain (P12729) and on the independent deletions 3.2 and 7.2. **A**, primer pairs were for an amplicon spanning TMs 2-4 of SK. **B**, control primers amplified *Shaker* in all samples indicating that the RT reactions were good.

A. SK

KB P 3.2 7.2



B. *Shaker*

KB P 3.2 7.2

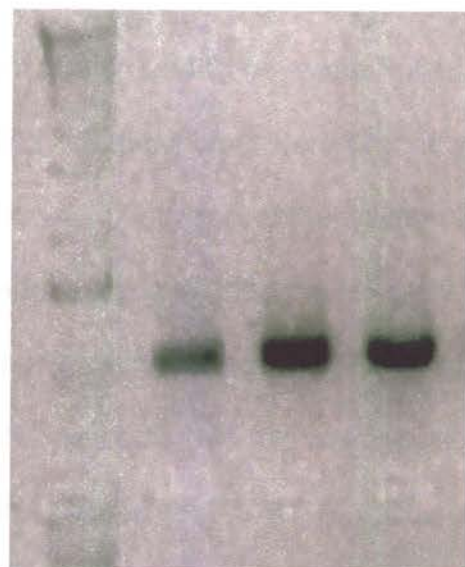


Figure 7

involving *Hobo* and P-elements¹³⁶. Release 3 of the annotated *Drosophila* genome sequence identifies the closest genes flanking the dSK gene as calcineurin (protein phosphatase 2B; CanB) and a potassium/amino acid transporter (CG3252). RT-PCR showed that the transcripts of these genes remain intact in both 3.2 and 7.2 strains (not shown).

Northern Blot and analysis of dSK RNA

Northern blots were prepared using total RNA samples from Canton S wild-type flies, P12729 flies (the P-element strain used to generate null mutants), and both dSK null lines, dSK3.2 and dSK7.2. Identical blots were probed with two separate ribonucleotide probes. One probe was contained entirely within the dSK null deletions representing exons 3-6, and a second probe was derived from sequences outside the deleted region representing exons 8-13 (see Appendix Item C). For the two probes, Canton S RNA samples had two major bands at 10 and 9kb (Figure 8), corresponding to the two largest 5' UTR splice variants differing approximately by the amount observed in RACE (see Appendix Figure B). The P12729 RNA sample had an identical hybridizing band pattern with a similar intensity as Canton S. Both of the dSK null RNA samples had no hybridization signal for the probe that was derived from sequences entirely within the deletion, but had a single band of 7.5kb for the probe derived from sequences outside the deletion. Therefore transcription does produce an mRNA from the mutant dSK allele but this transcript could not create a functional dSK

Figure 8: Total RNA from 50 adult flies probed with anti-sense ribo-probes representing: **A**, Transcript within the 44kb deletion, exons 3-6. **B**, Transcript outside the 44 kb deletion, exons 8-13. SK null flies do not contain transcripts containing essential transmembrane segments 1-5 and pore A. The null flies do, however, have a transcript that initiates at an unknown site and contains message for exons 8-13.

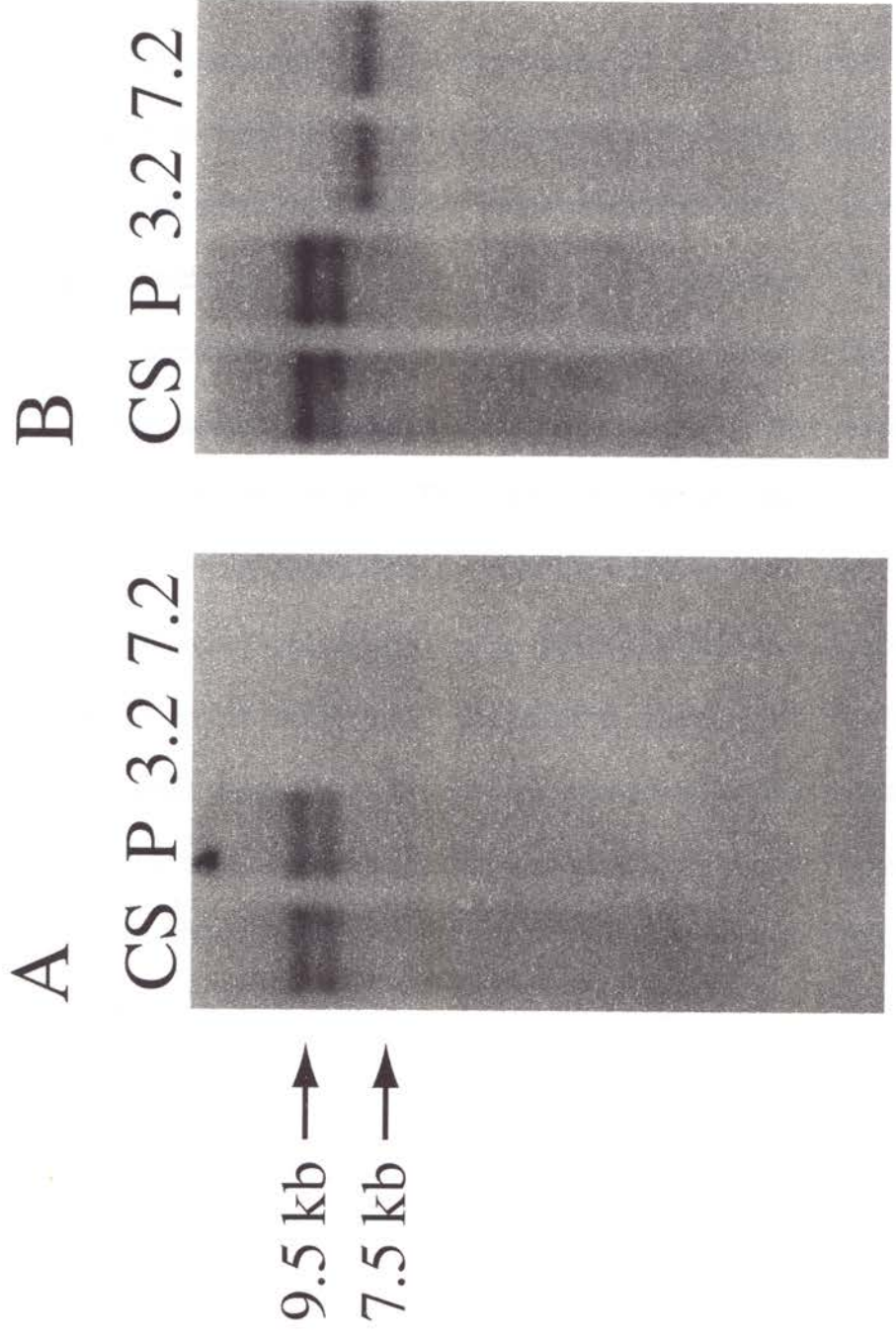


Figure 8

channel, as it does not code for transmembrane segments 1-6, which are required for channel function.

Behavioral analysis of dSK-null flies

Transheterozygotes of mutant strains 3.2 and 7.2 were compared to control flies (P-element strain with a precise excision) using classical behavioral assays such as adult flight escape, larval locomotor activity, larval phototaxis, courtship conditioning¹²², *Shaker* like ether sensitivity¹⁷, sticky feet¹³⁷, temperature sensitivity¹³⁸, and circadian activity (performed by Jaramillo)¹³⁹. None of these assays revealed behavioral phenotypes that were significantly different from control strains. The lack of positive data is not surprising considering that most *Drosophila* ion channel mutants were discovered using a forward genetic screen for deficiencies in motor function, and so isolated mutants were guaranteed to have overt quantifiable phenotypes. Furthermore, the classical behavior assays were designed to quantify phenotypes that had already been observed, and not to reveal subtle, unseen phenotypes. Nevertheless, we could not quantify a significant behavioral distinction between dSK-null flies and wild-type flies.

dSK mRNA characterization

In situ hybridizations were performed on embryos, larval fillets, larval brains, and adult brains using several dSK ribonucleotide probes. All probes gave only faint background signal that was also seen in dSK null strains (not

shown). Ribo probes were also incubated with the appropriate tissue from dSK nulls in attempt to pre-clear any background hybridization. These pre-cleared probes gave results similar to those that had not been pre-cleared.

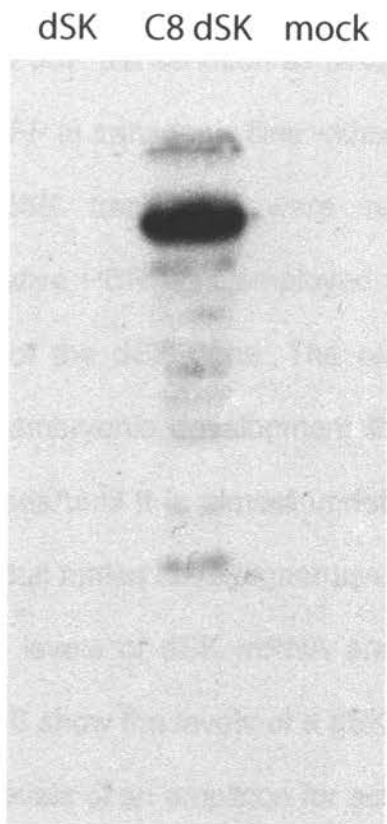
Antibodies were raised in rabbits, rats, and guinea pigs against several dSK epitopes (see Appendix Figure A). Two fusion proteins were sent to the Pocono Rabbit Farm for injection into rats and guinea pigs. Two peptides were synthesized and subsequently injected into rabbits by Global Peptide. Some of these antibodies detected the dSK protein by Western blotting of the expressed protein from transfected cells (Figure 9), but were not able to convincingly detect the native dSK protein either by Western blotting or immunohistochemistry (not shown). Western blots were performed on protein extracts from embryos, larvae, adult flies, and isolated adult heads. Immunohistochemistry was performed on embryos, larval fillets, larval brains, and adult brains using the Vectastain ABC Kit (Vector Labs, Burlingame, CA).

In order to decrease background signal, antibodies that successfully detected dSK expressed in Cos7 cells were affinity purified with the respective antigen. Purification did not improve antibody performance on native tissues as assayed above. Antibodies were also pre-cleared using tissue from dSK null flies or using Western blotted protein extracts from dSK null flies. Pre-clearing did not improve antibody performance as assayed above.

In situ hybridization and histochemical antibody staining were successful using control probes or sera for other *Drosophila* ion channels, confirming the efficacy of the techniques. It is possible that the dSK transcript and protein levels

Figure 9: Generating dSK antibodies. Rabbit polyclonal antibodies were raised (Global Peptide) against the exon 3 peptide GNTSRKPSTNSAKHKP. Cos7 cells were transfected with dSK or dSK containing the C8 epitope. Transfected cells were lysed and run as a western blot. **A**, anti-C8 binds to the expressed dSK-C8 protein. **B**, dSK antibodies detect Cos7 cell expressed dSK, with little background in mock-transfected lysates. Custom dSK antibody signal (chemiluminescent) develops faster than the commercially available C8 antibody signal. The dSK antibody, however, was not able to detect any differences between null and wild-type *Drosophila* head protein (or total protein, both not shown). Four other antibodies (two against peptides and two against fusion proteins) were as good or better than the one depicted.

A. anti-C8



B. anti-dSK

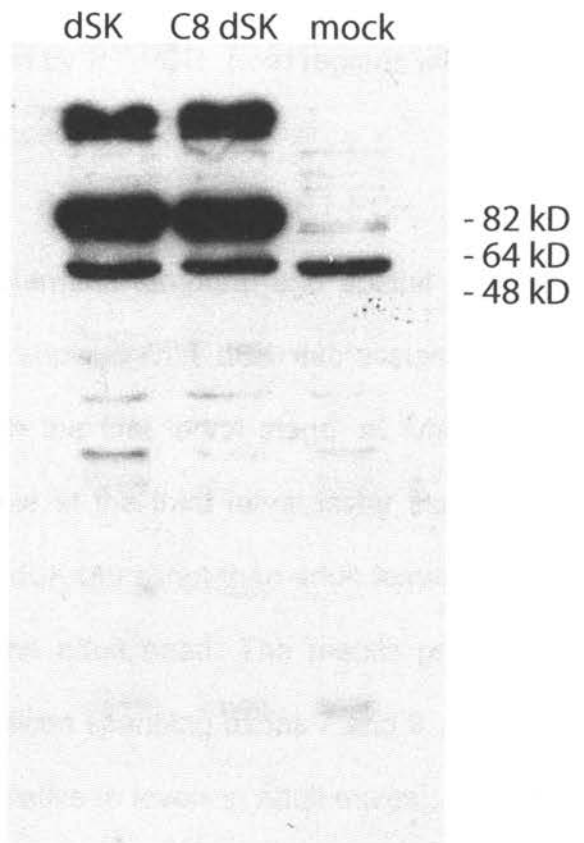


Figure 9

are below the detection limit of traditional methods. Attempts were also made to isolate dSK promoter sequence and use it to drive GFP expression in transgenic flies (as discussed previously). Promoter fragments were considered valid candidates when their deletion (accomplished by transposase excision) altered expression of dSK transcripts. Two regions (Figure 5) were identified that affected dSK transcription as determined by RT-PCR. Both regions were used to drive GFP in transgenic flies without success.

dSK transcripts were readily detected using RT-PCR. Therefore, quantitative PCR was employed to determine temporal and spatial expression profile of the dSK gene. The results showed that dSK expression increases during embryonic development through the first larval stage, at which point it decreases until it is almost undetectable at the third larval instar stage (Figure 10). Adult males have higher levels of dSK transcript than adult females and the highest levels of dSK mRNA are in the adult head. The results presented in figure 10 show the levels of a dSK amplicon spanning exons 7 and 8, normalized to the levels of an amplicon for actin (relative to levels in adult males). Consistent results were obtained using a separate dSK amplicon normalized to a separate housekeeping gene, ribosomal protein 49 (not shown).

Heterologous dSK expression

To measure dSK channel activity several splice variants were expressed in Cos7 cells, CHO cells, *Drosophila* S2 cells, and *Xenopus* oocytes. In all cases, heterologous dSK expression yielded whole-cell currents that were not different

Figure 10: Quantitative PCR. Temporal and spatial expression profile of dSK mRNA depicted relative to the level found in adult males, normalized to the levels of actin mRNA in each sample ¹²⁵. Error bars represent \pm standard deviations.

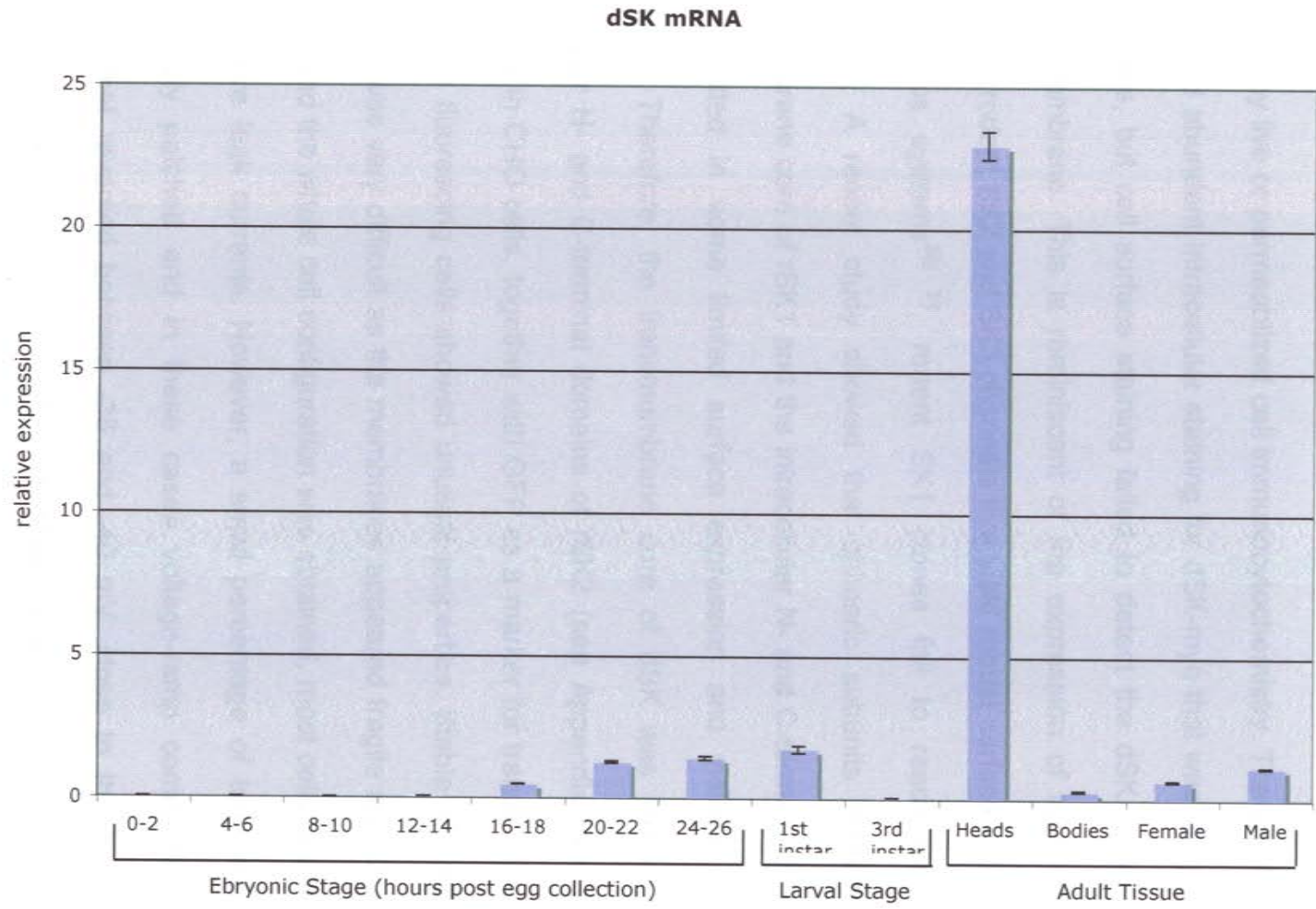


Figure 10

from control cells (not shown). To determine whether the dSK protein was being synthesized, a triple myc epitope was inserted into the extracellular loop between transmembrane segments 3 and 4⁷⁷, and dSK-myc transfected Cos7 cells were examined by live or permeabilized cell immunocytochemistry. The results (Figure 11) showed abundant intracellular staining for dSK-myc that was not present in control cells, but cell surface staining failed to detect the dSK protein at the plasma membrane. This is reminiscent of the expression of rodent SK1. In contrast to rodent SK2 and SK3 channels that yield robust surface expression in heterologous systems^{20; 71}, rodent SK1 clones fail to reach the plasma membrane. A recent study showed that chimeric subunits containing the transmembrane core of rSK1 and the intracellular N- and C-terminal domains of rSK2 resulted in some limited surface expression and yielded small SK currents⁷¹. Therefore, the transmembrane core of dSK was flanked by the intracellular N- and C-terminal domains of rSK2 (see Appendix Item B), then expressed in CHO cells, together with GFP as a marker for transfection (Figure 11). Green fluorescing cells showed unusual properties. Stable gigaseal patch formation was very difficult as the membranes appeared fragile and when seals did form and the whole cell configuration was obtained, most cells showed large nonselective leak currents. However, a small percentage of transfected cells were stably patched and in these cases voltage-ramp commands evoked currents that reversed between -38 and -40 mV, close to the expected K⁺ reversal potential under the recording conditions employed. The currents were partially blocked by TEA (50 mM; Figure 12), but not by apamin (100 nM) or d-

Figure 11: Cos7 cells transfected with dSK containing a triple MYC epitope tag in the 3-4 extracellular loop along with GFP on a separate plasmid as a transfection marker. Control cells were transfected with GFP and with dSK lacking the epitope tag. Cells were either left intact and stained, revealing surface expression, or permeabilized and stained, showing total expression. All channel constructs are expressed and detected with the MYC antibody (right panel). Only rSK2 MYC is detected on the cell surface (left panel). Both dSK and mSK1 show no surface expression.

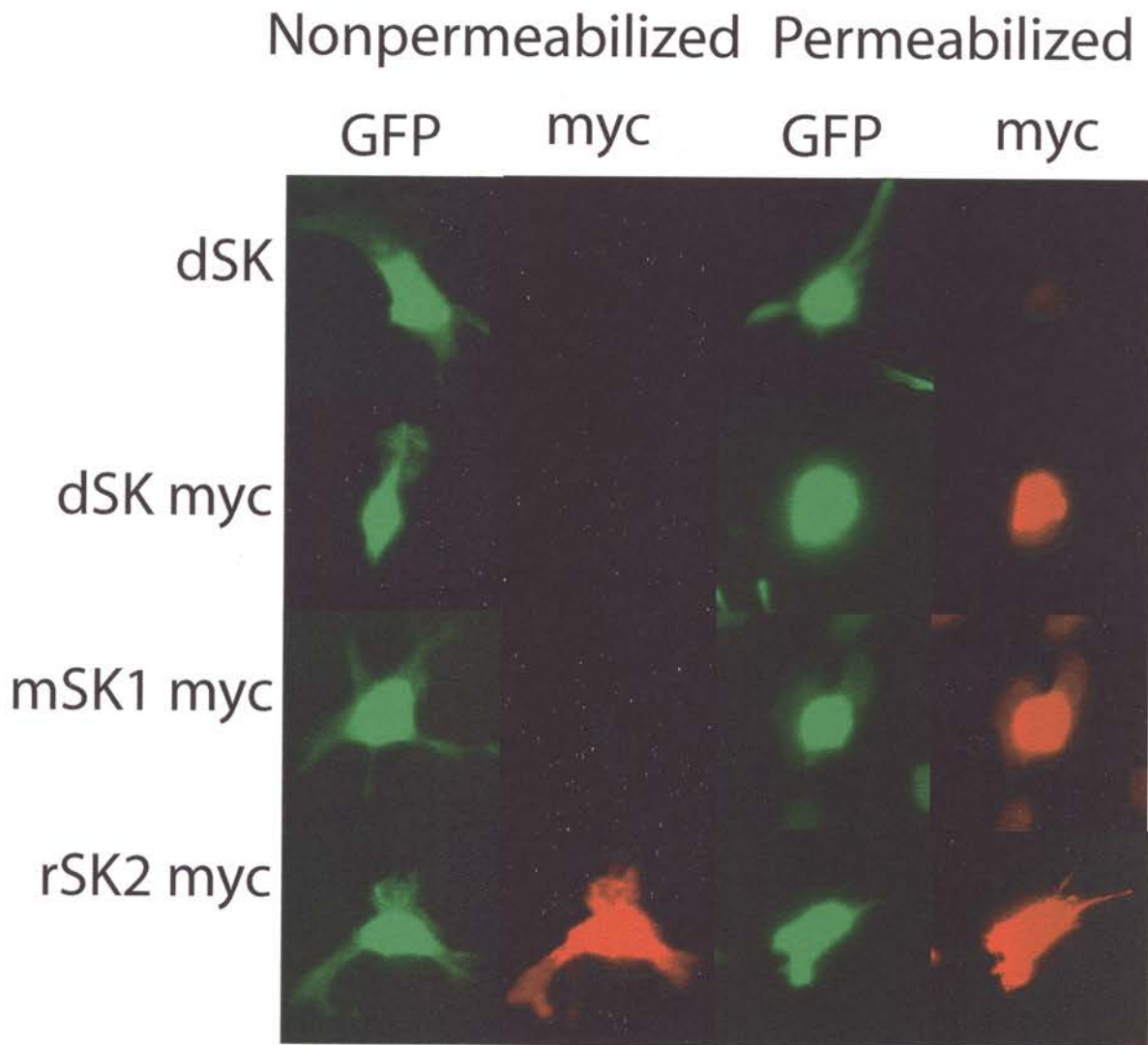


Figure 11

Figure 12: Chimeras of dSK with rSK2 (see Appendix Item B). Traces are current responses of CHO cells, in the whole cell configuration, to voltage ramp commands. **A**, CHO cells transfected with wild type rSK2 give current responses in the presence of 200 μ M intracellular CaCl_2 which are blocked by 50 mM TEA. CHO cells transfected with a dSK/rSK2 chimera give current responses in the presence of 200 μ M intracellular CaCl_2 , **B** and in the presence of 5 mM intracellular EGTA, **C**. Current responses in **B** and **C** are blocked by 50 mM TEA.

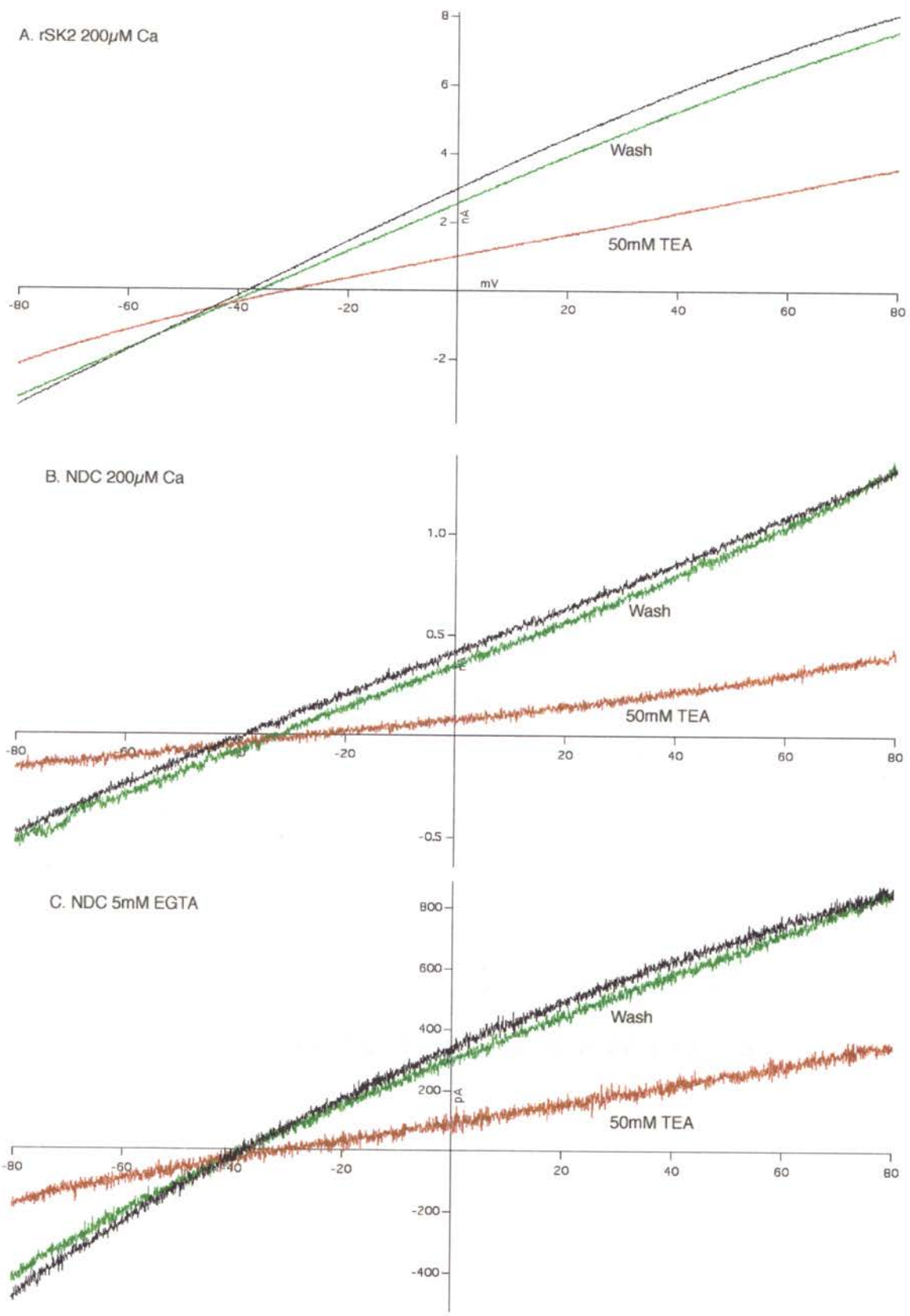


Figure 12

tubocurarine (50 μ M) (not shown) that effectively blocked control, rSK2 currents (not shown). Importantly, currents from cells transfected with dSK-rSK2 chimeras were observed either with or without Ca^{2+} in the internal solution (Figure 12). Based upon a K^+ current present only in transfected cells and block by the generic K^+ channel blocker, TEA, these results suggest that the transmembrane core of dSK can be trafficked to the plasma membrane but it does not function as a typical SK channel when flanked by the intracellular domains of rSK2 that contain the Ca^{2+} gating machinery of the channel.

Epitope tagged (V5) dSK was also expressed in *Drosophila* S2 cells. Lysates of S2 cells were prepared as western blots, but dSK protein could not be detected with the V5 epitope antibody or with the dSK antibody (Figure 13). dSK, both tagged and untagged, however, was detected in lysates of transfected Cos7 (Figure 11) and CHO cells. rSK2 expresses robustly in S2 cells (Figure 13) and produces functional channels (not shown). Constructs were also made with epitope-tagged and untagged dSK for overexpression in transgenic flies (as previously discussed). Transgenic flies (injections performed by Duke MSG) integrating these constructs were designed to express dSK driven by the strong *Drosophila* actin promoter and neuronal *elav*. Positive transformants were confirmed by genomic PCR, but failed to produce SK message (RT-PCR) or protein (western blot).

Figure 13: *Drosophila* S2 cells were stably transfected with dSK, rSK2, dSK-MYC, or rSK2-MYC. All constructs also contained the V5 epitope. Western blots of S2 cell lysates probed with the V5 antibody show that S2 cells will express rSK2 channels but not dSK channels. This result is odd because mammalian cells express dSK (Figures 9 and 11).

Anti-V5

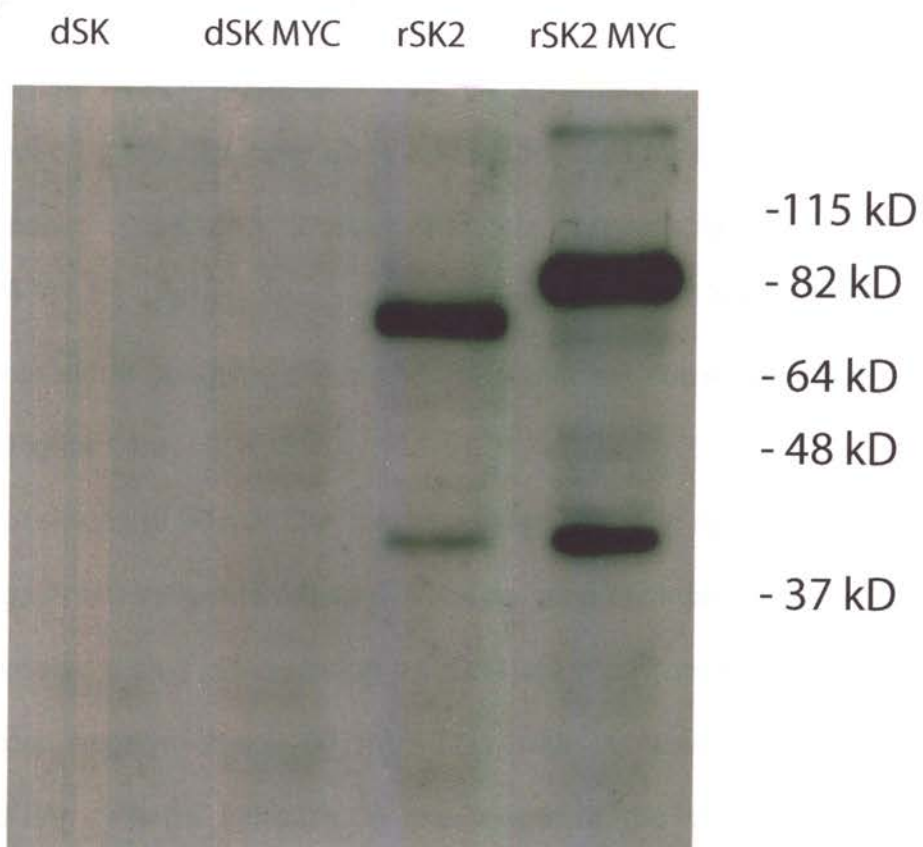


Figure 13

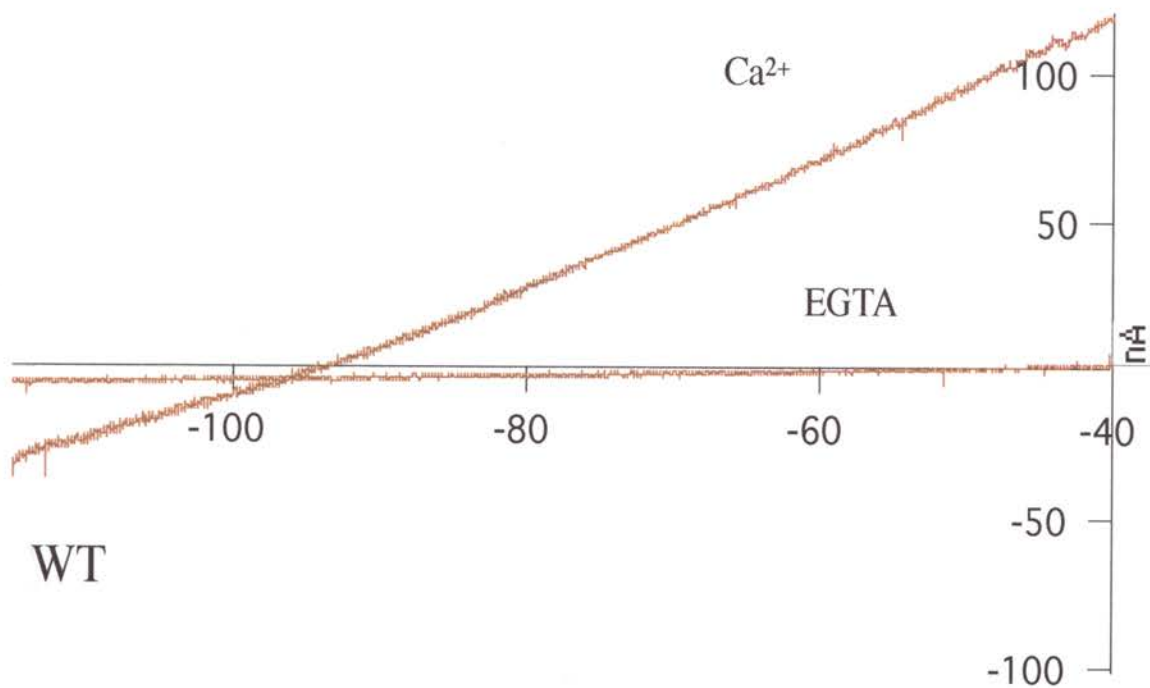
Larval Muscle Recordings

To determine whether dSK channel activity underlies I_{CS} , voltage-clamp recordings were performed from wild-type and dSK-null ventro-lateral longitudinal muscle fibers of the third instar larvae (assisted by Timothy Strassmaier). To isolate I_{CS} , muscle cells were voltage clamped at -80 mV and 2 second voltage ramp commands from -100 to -40 mV were delivered in the presence or absence of extracellular Ca^{2+} . In this voltage range the Ca^{2+} - and voltage-activated BK channel encoded by the *Slowpoke* gene and responsible for I_{CF} ¹⁴⁰, or the strictly voltage-dependent *Shab* and *Shaker* channels responsible for I_K and I_A , respectively^{16; 141; 142}, will not be appreciably activated. Ca^{2+} -free bath solution recordings from either genotype did not reveal significant currents between -100 and -40 mV (Figure 14a).

Upon perfusion of 20 mM Ca^{2+} under voltage clamp at -80 mV, the holding current changed from inward to outward. Voltage-ramp commands from -110 mV to -40 mV revealed a shift in the resting reversal potential from around -45 mV to potentials more negative than -80 mV. This shift in reversal potential was accompanied by a large increase in the slope of the current responses, suggesting that the addition of Ca^{2+} was leading to the opening of a potassium conductance, presumably I_{CS} (Figure 14). Presumably calcium entered the muscle cell through voltage-activated calcium channels activated by ramp commands. Indeed, the reversal potential of this calcium-dependent current shifted predictably with changes in extracellular $[K^+]$. This Ca^{2+} -dependent

Figure 14: Two electrode voltage clamp recordings of larval muscle with or without bath applied Ca^{2+} . Electrodes had a tip resistance of 5-7 mega ohms. Larva were bathed at 4° C in the following Ca^{2+} free recording solution: 128 mM NaCl, 2mM KCl, 20 mM MgCl_2 , 75.5 mM Sucrose, 5 mM HEPES, and 0.5 mM EGTA. Cells were held at -80 mV prior to voltage ramps from -110 to -40. After the first ramp the bath solution was exchanged with one containing Ca^{2+} (4 mM MgCl_2 , and 20 mM CaCl_2). Representative traces for wild-type Canton S flies, **A** and dSK null isolate 7.2 flies, **B**. Both panels show the first and tenth ramp, Calcium caused a shift in reversal potential and a large increase in slope of the current- voltage traces. The reversal potential of this calcium-dependent current shifted predictably with changes in extracellular $[\text{K}^+]$ (not shown).

A



B

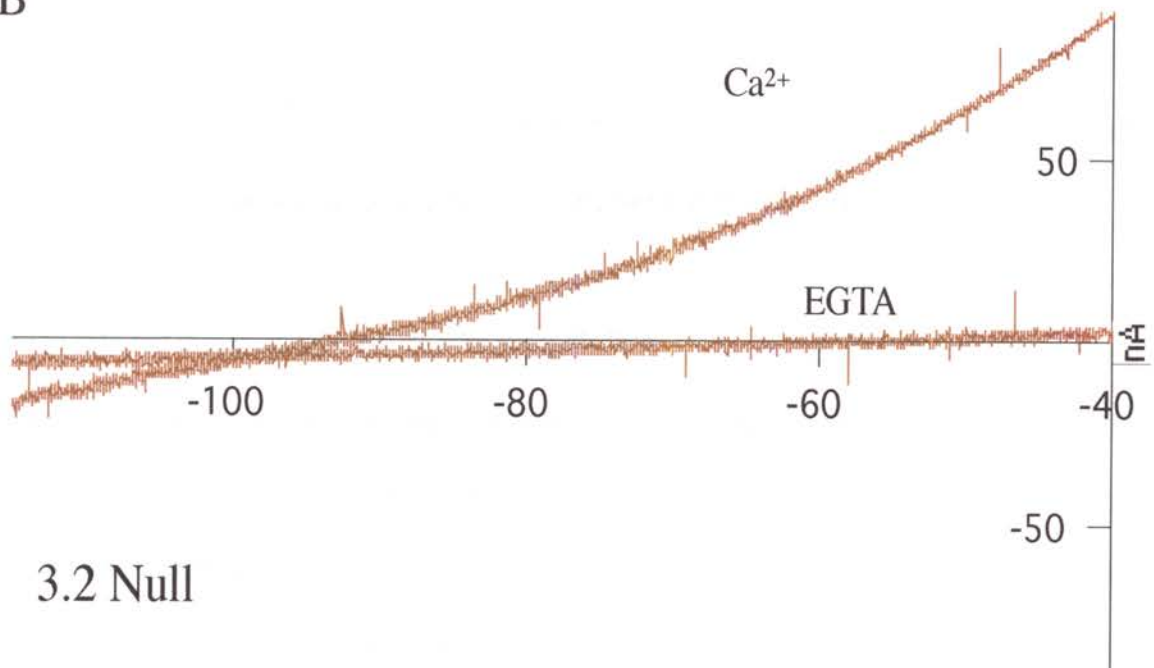


Figure 14

current cannot be attributed to either the B channel, Slowpoke, or to dSK as this current was observed in *Slowpoke* (not shown) and dSK-null larvae (Figure 14b).

In Ca^{2+} -containing bath solution, approximately linear currents were evoked that reversed at ~ -90 mV, close to the presumed K^+ reversal potential. These Ca^{2+} -dependent currents were seen in both wild-type and dSK null flies. Therefore, it is likely that dSK channels are not responsible for I_{CS} and the molecular identity of the I_{CS} channels remains to be determined.

Summary of Results

We have shown the structure of the single SK channel gene in the *Drosophila* genome, dSK. The gene spans at least 80kb and contains at least 13 coding exons. Several splice variants were found including two variant pore exons with predicted coding sequence distinctions in the selectivity filter that suggest functional consequences. The transmembrane core of the channel is highly homologous to the mammalian SK channels as is the CaMBD, suggesting a conserved mechanism for Ca^{2+} gating^{62; 65; 66}. Two independent dSK null lines were generated by imprecise gamma ray P-element mobilization. RT-PCR, Northern blotting, and DNA sequence analysis verified that the genomic alterations abolished expression of a functional dSK protein, eliminating the transmembrane core of the channel, yet leaving flanking genes intact. Although we failed to detect dSK protein in wild-type flies, quantitative RT-PCR demonstrated that the dSK mRNA is developmentally regulated and expressed in

the adult fly brain. Despite this expression, behavioral analyses did not reveal an overt phenotype for either of the two independently derived dSK null lines.

Mammals have four genes that code for unique but homologous SK channel subunits. The sequenced *Drosophila* genome has only one SK channel gene that is most similar to mammalian SK1. In contrast to mammalian SK2 and SK3, little insight has been gained into the physiological roles of SK1. Like dSK, heterologous expression of rodent SK1 results in channel proteins that are not trafficked to the plasma membrane. Cells heterologously expressing the dSK protein were notably fragile and unhealthy (most likely due to lack of calcium gating see below). For both dSK and rSK1, flanking the transmembrane core of the protein with the intracellular domains from SK2, a channel that is readily trafficked to the plasma membrane, resulted in limited cell surface expression and functional channels. For dSK the evidence for functional chimeric channels is that currents reversing at the expected K^+ reversal potential were only seen in transfected cells, and these currents were blocked by TEA. Unlike rSK1-rSK2 chimeric channels, chimeric dSK-rSK2 channels were not Ca^{2+} -gated. This may reflect differences in the coupling between the CaMBD and the core of the protein, particularly interactions between the flexible linker N-terminal to the CaMBD and the S4-S5 loop (unpublished observations). There is strong evidence for recordings of native SK2¹⁰⁸, SK3^{143; 144}, and IK1 (SK4) channel activity^{145; 146}, while no recordings have been attributed to native rodent SK1 channel activity. Similarly, in *Drosophila*, no recordings can convincingly be attributed to dSK channel activity. Knockout mice have been created for each of

the mouse SK channel genes. SK2-null, SK3-null^{108; 109}, and IK1-null mice¹⁴⁷ have multiple overt phenotypes, yet no clear phenotype has yet emerged from SK1-null mice (unpublished observation). Taken together with the lack of surface expression, it is possible that dSK channels perform their physiological role on the membranes of intracellular organelles, or that these channels require an auxiliary, associated subunit for proper trafficking to the cell surface and ion channel function.

Chapter IV. Discussion

dSK null flies generated in this research project did not display overt behavioral phenotypes. This discussion of the project will address two major questions that arise from the negative results. First, given the extensive track record of *Drosophila* as a research organism should we have expected a phenotype? Numerous forward genetic screens for neurological mutants have been performed and none have identified SK. Genes identified in such screens show up many times in the literature with multiple alleles. Furthermore, electrophysiological recordings from *in vivo* preparations have not identified a current or potential that has the properties of the characterized mammalian channels. Lastly, mice null for SK1, the rodent gene most similar to dSK, do not display phenotypes either. The second question that arises is, since dSK is not involved in overt processes what subtle function could it be performing?

Saturation Mutagenesis

The use of *Drosophila* as model system for the study of genetics began in 1910 in the laboratory of T. H. Morgan¹⁴⁸. In the beginning mutations were single, spontaneous or induced events that were isolated and observed one at a time. The first example of a genome wide screen designed to identify all genes required for a specific biological process occurred in 1980 when Nusslein-Volhard and Wieschaus performed a forward genetic screen for mutations affecting segment number and polarity¹⁴⁹. This study resulted in an explosion of

forward genetic screens and a subsequent Nobel Prize (for the concept originators). The first of many screens for behavioral mutants was soon to follow¹⁵⁰. However, no screen to date has identified a behavioral phenotype for mutation in the SK locus. The general consensus is that of the approximately 13,600 *Drosophila* genes only about 20% have null phenotypes that have been discovered¹⁵¹. Of that 13,600, however, only one third is expected to have overt null phenotypes, with the remaining two thirds being aphenotypic¹⁵². Geneticists are only recently confronting the question of how to deal with these aphenotypic loci¹⁵³.

The method of mutagenesis that has been the most successful by far, in terms of quantity, is P-element disruption¹²¹. Although this method is not targeted it is not random either. Hot and cold spots of integration have been identified. One could argue that it is a game of numbers and SK has not received a mutational hit yet, or that SK lies in a cold spot that is not available to P-element disruption. As a reference one can look at the example of the *Shaker* gene. This gene is known to have an overt phenotype, and behavioral screens over the years have isolated 41 separate behavioral alleles recorded in Flybase. A glance at the annotation of the SK gene on Flybase shows that there are fifteen P-element insertions in the SK gene, most of which should disrupt transcription, but none have associated phenotypes. The results of this study agree, indicating that disrupting the SK gene does not result in an observable phenotype. SK must belong to the population of genes that does not have an overt null phenotype.

Well Characterized *In Vivo* Preparations

On a cellular level the physiology of ion channels is studied through electrical recording. The *Drosophila* model system has a rich history of ion channel physiology. There are four classic *in vivo* preparations, cultured giant neurons¹⁵⁴, larval body wall muscle¹⁵⁵, pupal muscle¹⁵⁶, and adult indirect flight muscle¹⁵⁷. The stereotypical line of research begins with an isolated neurological mutant. The mutant is shown to be defective in or lacking of a conductance or potential (from one of the four preparations above) that has previously been characterized as having unique kinetic and/or pharmacological properties. From this mutant the genetic lesion and nucleic acid sequence coding for the wild-type channel protein is deduced. This approach has been so successful that almost every unique *in vivo* current has been accounted for with a respective behavioral mutant and underlying mutant channel sequence. The potassium channel family in particular has been exhaustively studied. Four main potassium conductances have been identified and are common to all of the *in vivo* preparations: the voltage-activated potassium conductances I_A and I_K and the calcium-activated potassium conductances I_{CF} and I_{CS} . I_A is rapidly voltage activated and inactivates rapidly as well. The *Shaker* channel carries the majority of this conductance 18, with a small portion mediated by *Shal* (the percent contribution of *Shaker* and *Shal* varies among the four classical preparations)¹⁵⁸. I_K activates more slowly but does not inactivate and persists for the duration of a voltage pulse. The *Shab* and *Shaw* channels account for this current¹⁵⁹. I_{CF} is rapidly

activated by voltage and calcium; this conductance also inactivates rapidly. The *Slowpoke* channel has been shown to be responsible for I_{CF} ¹⁶⁰. The remaining current, I_{CS} , is activated by calcium only and has slow kinetics. The channel behind this conductance has not yet been identified. Cloned mammalian SK channels activate rapidly in response to calcium so it is not likely that dSK is responsible for this slowly activating conductance. Furthermore, the larval muscle preparation of dSK nulls still possesses a current that is probably I_{CS} (Figure 14).

No Phenotype for Rodent SK1

Of the four mouse clones *Drosophila* SK sequence is most similar to mSK1. The similarities do not stop there. Neither dSK nor mSK1 have been convincingly recorded *in vivo* or in heterologous systems. Neither channel reaches the cell surface when expressed in cultured cells. Mice and flies null for the genes do not display overt phenotypes, and preparations from both null organisms still contain currents that were previously (but erroneously) ascribed to the clones^{69; 161}.

As discussed above, the only *in vivo Drosophila* conductance without an associated channel clone is the I_{CS} . This current is most similar to the mammalian slow afterhyperpolarizing current (I_{sAHP}). Both the I_{CS} and the I_{sAHP} are activated by intracellular calcium (directly or indirectly) and are voltage independent^{119; 162}. The kinetics of both currents are similar in that both activate slowly (seconds) in response to calcium. The I_{sAHP} is modulated by second

messengers such as cyclic AMP¹⁶³, and the I_{CS} is significantly different in mutants that effect cAMP levels^{164; 165}. Furthermore TEA blocks both currents^{166; 167}. The I_{CS} and the I_{sAHP} may be orthologous currents, but their kinetic properties do not match those of cloned SK channels, and current evidence fairly convincingly shows that they are not carried by SK channels^{108; 162}. With the I_{CS} and I_{sAHP} out ruled there are no other plausible candidates for in vivo recordings of dSK and mSK1.

Neither mSK1 nor dSK has been recorded from in heterologous system and it appears that they do not even traffic to the cell surface. The present study expressed dSK in the mammalian cell lines Cos-7 and CHO and the *Drosophila* S2 cell line. Previous studies in the lab observed dSK in xenopus oocytes. The laboratory has also attempted to express mouse and rat SK1 in the same heterologous systems (save S2). None of these attempts have produced successful recordings. The literature also lacks any successful expression of dSK or rodent SK1 except for one study that uses the N and C terminus of SK2 to drag the core transmembrane region SK1 to the surface⁷¹. We made a similar chimera with dSK in this study producing similar results (Figure 12). When dSK and mSK1 were tagged with an extracellular epitope and expressed in Cos-7 cells, surface staining showed that the channels do not leave the endoplasmic reticulum (Figure 11). *Drosophila* SK was also expressed in the S2 cell line with no recorded currents. Expression of epitope tagged dSK and rSK2 showed that the problem is much more severe in the *Drosophila* S2 cell line. Western blotted

protein extracts indicated that S2 cells produce full-length rSK2, but fail to produce any dSK protein (Figure 13).

Lastly, null mice have been generated for all four mammalian SK clones. SK2, 3, and 4 null mice display overt phenotypes that have been reported in the literature¹⁰⁷⁻¹⁰⁹. Mice null for SK1 have been extensively studied in the Adelman lab, but no phenotype has been observed to date. PCR studies of SK2, 3 and 4 message levels in SK1 null mice show that none of the other SK transcripts are upregulated in a compensatory fashion¹⁰⁸. SK1 null mice have also been sent out to other labs that have been unable to observe a phenotype. The story is again the same with dSK null flies as we have been unable to detect functional consequence of gene deletion.

Possible Roles

In SK1 null mice no neurological defects have been detected. One could argue that SK2 and 3 compensate for the loss of SK1 function. In *Drosophila* this argument does not fly (sorry) because there is only one SK gene. SK null flies are not lethal, in fact they appear to function as well as wild type flies. One might conclude that the SK gene is not necessary at all in *Drosophila*. True, it is not necessary in laboratory culture conditions, but phylogenetic conservation dictates that there is selective pressure and therefore some advantage to having the SK gene. Two possibilities exist. First, dSK could be redundant in flies but that would mean that a potassium channel outside the SK family covers the deletion. Second, dSK function is only required in extreme conditions that are not

encountered in laboratory culture conditions. The next section of this discussion will discuss these two possibilities.

Another Potassium Channel Covers the *Drosophila* SK Mutation

When creating an organism with a classical null allele, one fundamental problem arises: the gene in question is not removed minutes before any assays are performed on the mutant. The gene is absent from the single cell stage and homeostatic compensation starts at that point. In extreme cases mutants have compensatory changes that can be seen structurally, but lack any overt behavioral phenotypes¹⁶⁸. Organisms functionally compensate for a genetic lesion using any means possible to return to equilibrium. Accordingly when an SK channel gene is deleted, the fly may respond by aberrantly expressing another potassium channel where dSK is usually expressed. For this hypothesis to be viable there must be a suitable channel replacement. Some might only look to voltage-independent, small-conductance, calcium-activated potassium channels. Others may be less strict and only require that the replacement be a potassium channel. Of course it is more likely that the replacement channel has properties similar to SK, but a modern understanding of Biology where rules are constantly broken does not require it.

Two candidate potassium channels that might functionally cover for the SK channel are the *slowpoke* channel and the *eag* channel. The *slowpoke* channel is a potassium channel that, like SK, is calcium modulated. Unlike SK it requires calcium and voltage, acting as coactivators. The *slowpoke* channel also

has a much larger unit conductance than SK channels. This difference in conductance could be overcome in a genetic compensation scenario by expressing *slowpoke* at lower levels than SK, resulting in similar amounts of total current. Besides the fact that both channels are activated by calcium, studies in *Drosophila* provide no other evidence that *slowpoke* may be providing redundant function. For example little is known about the expression profiles of SK and *slowpoke*. Studies in rodents, however, show that both channels are involved in generating the afterhyperpolarization (AHP as discussed in the introduction). SK2 and BK (mammalian homolog to *slowpoke*) contribute to different kinetic components of the AHP, but many accessory protein subunits are known to regulate the components of *slowpoke*/BK³⁸. If dSK is involved in the AHP in an as yet identified cell type in *Drosophila*, one could functionally substitute *slowpoke*, expressed at lower levels to account for the conductance difference and with altered kinetics achieved through accessory proteins.

The other possible functional replacement is the enigmatic *ether-á-go-go* (*eag*) channel. This behavioral mutant and the underlying potassium channel get their name from the leg shaking phenotype observed when *eag* flies recover from ether anesthesia¹⁷. The *eag* locus was identified because of its similarity to the *shaker* gene¹⁶⁹; both are potassium channel alpha subunits with six transmembrane/reentrant pore-loop architecture. Typical potassium channel mutants affect a single conductance that is defined by unique kinetic and pharmacological properties. *Eag* mutants are different from most of the classic potassium channel mutants because they affect multiple potassium currents. All

four of the classic potassium conductances in larval muscle, I_A , I_K , I_{CF} , and I_{CS} are reduced in *eag* mutants¹⁷⁰. Before *eag* was well studied there was an apparent one-to-one correspondence between channel proteins and separable potassium currents. *Eag* mutants show that the situation might not be as simple as it was initially assumed. Native potassium channels might be heteromeric proteins with subunits from multiple channel families. What were initially presumed to be the essential alpha subunits might be modifier subunits to an *eag*, *elk* (*ether-á-go-go like*), or *erg* (*ether-á-go-go related gene*) core. The native “SK” channel could be heteromultimer made up of SK and *eag* alpha subunits. The central hypothesis being that conduction can be achieved with the *eag* alpha subunit alone in a homomer, and the SK alpha subunit is not required for survival in laboratory conditions. Of course, this line of thinking need not even involve *eag*, and will be discussed further in the next section.

Drosophila SK, Only Required for “Extreme Circumstances”

It is possible that *Drosophila* SK is not necessary for flies to thrive in the laboratory environment. In the laboratory food is constantly available and temperature, humidity, oxygen levels are maintained within acceptable levels. Culture conditions are designed to propagate all stocks, weak and strong alike. Flies in the wild, however, deal with a wide range of extreme environments. The narrow range of experiences encountered in the laboratory only requires a narrow subset of the full genetic compliment. In the wild, when adverse conditions arise, the organism can call upon stress response systems designed

to deal with them, and there are a few options for regulating these systems. System components could exist as fully mature proteins, precursor proteins, mRNA, or simply chromosomal DNA. Of course maintaining a standby stock of mature proteins or even mRNA is metabolically wasteful. For that reason most products of stress response systems are transcribed and translated in response to adverse stimuli¹⁷¹. One classic example is the heat shock response system. Discovered in yeast, this system initiates the transcription of chaperone proteins in response to unfavorable temperature extremes. Heat causes proteins to denature, the chaperones guide their refolding, restoring function. Many of the heat shock proteins produced by this response system are undetectable under normal yeast culture conditions. Is it possible that SK exists as a component of some stress response system?

At all stages of *Drosophila* development, under normal laboratory conditions we have been unable to detect SK protein. Messenger RNA is detectable by Northern blot analysis and RT-PCR, but controls performed during both experiments indicate that the message exists at low levels. Although suggestive, this is hardly direct evidence that SK is part of some stress response system. A recent paper by the group of Susan Celniker, however, provides evidence validating the stress response system hypothesis¹⁷². This paper compares the fully sequenced *Drosophila* genome with cDNA and EST (expresses sequence tag) sequence. Most mRNA sequence (as reported by cDNA and EST) matches perfectly with the genomic region encoding it. In some genes, however, there are clear cases of adenosine to inosine editing caused by

the RNA specific adenosine deaminase (ADAR). The Celniker group identified an ADAR edited site in the calmodulin binding domain (CaMBD) of dSK, which changes a tyrosine codon to a cysteine codon¹⁷². Furthermore they made the observation that the edited tyrosine is involved Van der waals contacts with calmodulin as described in the crystal structure of this region in rSK2 62. Additionally, the site appears to be nearly completely edited throughout development. It is unclear if SK mRNAs with this change in the CaMBD will exit the nucleus for subsequent translation¹⁷³⁻¹⁷⁵, and if they are translated, do they bind apocalmodulin or gate in response to calcium in the typical fashion. It has been shown that in heterologous systems rSK2 channels without associated calmodulin subunits are not expressed on the cell surface⁷⁷. The list of genes edited by ADAR includes many genes involved in neurological processes^{176; 177}, and ADAR null flies, generated from a reverse genetic approach, display locomotor defects^{178; 179}. ADAR null flies were also generated in a forward genetic screen for flies that are sensitive to anoxia^{180; 181}. Because of these studies, I and others¹⁸² have assumed that ADAR plays a role in a heat shock like stress response system. Changes in the partial pressure of oxygen affect the extent to which RNA, possibly including SK, is edited. In this scenario, SK RNA would be edited and unable to bind calmodulin under normal conditions. Anoxic conditions might decrease ADAR activity, allowing transcription and translation of unedited, calmodulin binding SK. There are in fact examples of SK channels in mammalian systems being regulated by hypoxia^{183; 184}.

Intracellular Membranes

All attempts to express rodent SK1 and dSK in heterologous systems have resulted SK protein localized on intracellular membranes (Figure 11). Most who have encountered this result have assumed that SK channels always belong on the cell surface, and have worked towards that goal⁷¹. Not much thought has been given to the notion that native SK1 and dSK might be expressed on intracellular membranes. The work of Pedro Verdugo provides some insight into possible roles that SK channels might perform when and if they are expressed on intracellular membranes. In one paper, he shows that apamin can modulate calcium waves observed in isolated nuclei¹⁸⁵. The model he comes up with to explain this result requires that SK channels be expressed on intracellular membranes. The model theorizes that calcium induced calcium release from intracellular stores could be rapid and complete if a counter ion entered stores as calcium exited. Without a counter ion the process of calcium exiting stores would be electrogenic and therefore limited. Potassium is the logical choice for such a counter ion, as its intracellular concentration is high. SK channels on intracellular membranes might provide the conduction pathway for potassium counter ions. The same calcium that activates inositol triphosphate receptors (calcium induced calcium release channel) could activate SK channels. Finally the presence of SK channels on intracellular membranes would explain the observed apamin modulation of calcium waves¹⁸⁵. While this hypothesis is intriguing it presents some problems. First, apamin applied to isolated nuclei should not have access

to the appropriate face of SK channels unless it is actively transported inside the nuclei. Second, this hypothesis does not explain why dSK nulls are aphenotypic.

Chapter V. Summary and Conclusions

Forward vs. Reverse Genetics

After discussing dSK, a brief description of a common problem in the post genomic era seems prudent. In the past, the study of *Drosophila* mutants used a forward-genetic approach. In this method, an observed phenotype eventually led to the identification of the underlying gene. Since phenotypic mutants were observed before scientists had firm concept of what genes were, it makes sense that this direction of inquiry came first. Through the years the concept of what we mean by the word gene has changed dramatically. For pioneers of *Drosophila* research, the word might suggest a specific heritable trait. For those in the pre golden age (before Watson and Crick), the word gene might refer to the physical region on a chromosome responsible for that trait. Finally, in the genomic era, most of us think of a specific nucleic acid sequence that encodes products that effect that trait (micro RNAs being the exception). So this was the way our understanding of genetics progressed, the forward-genetic approach. An isolated phenotype was almost always guaranteed to lead to the discovery of an underlying gene. In the reverse-genetic approach common in the post genomic era, there are no such guarantees. The fact that observable, heritable phenotypes have genetic basis is one of the central tenants of science that has rarely been broken. We always know where to look for the end point of the forward-genetic approach: in the genes. Furthermore, this endpoint is always spelled out in the same language: DNA. The reverse-genetic approach taken

frequently in the post genomic era does not have the same luxuries. One usually begins by eliminating the gene and then looking for a phenotypic outcome. The problem is that the endpoint of the reverse approach is not in a universal language. In fact the endpoint is the entire range of experiences possible that may affect the fitness of a fly. The endpoint for reverse genetics is not a string of nucleic acids, it is nociception, gravitaxis, vision, memory, odor sensation, and so on.

Sometimes null organisms will not have overt phenotypes. Because of the upfront investment involved in generating the knockout organism, most researchers will push forward and attempt to reveal a phenotype. In *Drosophila* generating a null allele is moderately time consuming, but the initial investment is far greater when dealing with mice. The question becomes, “to knockout or not to knockout?” If one has preliminary data such as *in situ*, antibody staining, or evidence of *in vivo* function, the project might not be that risky. Preliminary data provides a framework for analyzing the mutant, narrowing the focus. If, however, a gene lacks any associated preliminary data, generating a null may be too large of an investment when considering the chances of failure. I feel that we currently lack the proper tools for exposing subtle phenotypes. The idea that aphenotypic genes might be involved in stress response systems was discussed above. This notion suggests that in the right environment an aphenotypic organism might perform differently than a wild-type organism. Some scientists have suggested screening environments on a high throughput scale¹⁵³. Sean Cutler, an arabidopsis geneticist, envisions a combination of chemical genetics¹⁸⁶ and a

generic lethal screen. Briefly, chemical genetics uses a library of chemical compounds to explore protein function. Cutler sees each chemical as a different environment. Wild type and aphenotypic organisms would be confronted with an effective library of environments. Presumably the aphenotypic mutant lacks a component of a stress response system designed for coping with one of the artificial environments and would display decreased fitness when exposed to that environment. Developing an appropriate standard array of chemicals would take time, but once established researchers could simply screen their aphenotypic mutant.

Some in the post genomic era have tools that narrow the focus of the reverse approach. Information such as an expression profile obtained through antibody staining or *in situ* hybridization is helpful. Information from studies on genes in the same family might catalyze a successful search for a phenotype. Nonetheless there appears to be a significant quantity of aphenotypic genes that exist. For those considering a reverse-genetic approach: proceed with caution and do not put all of your eggs in one basket.

Bibliography

1. Kandel, E.R., Schwartz, J.H., and Jessell, T.M. (2000). Principles of neural science, 4th edn (New York, McGraw-Hill, Health Professions Division).
2. Lloyd, G.E.R. (1970). Early Greek science: Thales to Aristotle (New York,, Norton).
3. Gilbert, W., and Wright, E. (1600). De magnete, magneticisque corporibus, et de magno magnete tellure; physiologia nova, plurimis & argumentis, & experimentis demonstrata (Londini,, Petrus Short).
4. Musschenbroek, P.v. (1739). Essai de physique (Leyden,).
5. Galvani, L. (1792). De viribus electricitatis in motu musculari (Mutinae,).
6. Ringer, S. (1883). A further Contribution regarding the influence of the different Constituents of the Blood on the Contraction of the Heart. The Journal of physiology 4, 29-42 23.
7. Seyfarth, E.A. (2006). Julius Bernstein (1839-1917): pioneer neurobiologist and biophysicist. Biological cybernetics 94, 2-8.
8. Bernstein, J. (1869). Ueber den zeitlichen Verlauf der negativen Schwankung des Nervenstroms. Pflugers Arch 1, 173-207.
9. Hodgkin, A.L., and Huxley, A.F. (1952). A quantitative description of membrane current and its application to conduction and excitation in nerve. The Journal of physiology 117, 500-544.

10. Hodgkin, A.L., and Katz, B. (1952). A quantitative description of membrane current and its application to conductance and excitation in nerve. *J Physiol* 117, 500-544.
11. Narahashi, T., Moore, J.W., and Scott, W.R. (1964). Tetrodotoxin Blockage Of Sodium Conductance Increase In Lobster Giant Axons. *The Journal of general physiology* 47, 965-974.
12. Armstrong, C.M., and Binstock, L. (1965). Anomalous Rectification In The Squid Giant Axon Injected With Tetraethylammonium Chloride. *The Journal of general physiology* 48, 859-872.
13. Doyle, D.A., Morais Cabral, J., Pfuetzner, R.A., Kuo, A., Gulbis, J.M., Cohen, S.L., Chait, B.T., and MacKinnon, R. (1998). The structure of the potassium channel: molecular basis of K⁺ conduction and selectivity [see comments]. *Science* 280, 69-77.
14. Gardos, G. (1958). The function of calcium in the potassium permeability of human erythrocytes. *Biochim Biophys Acta* 30, 653-654.
15. Noda, M., Shimizu, S., Tanabe, T., Takai, T., Kayano, T., Ikeda, T., Takahashi, Nakayama, H., Kanaoka, Y., Minamino, N., *et al.* (1984). Primary structure of *Electrophorus electricus* sodium channel deduced from cDNA sequence. *Nature* 312, 121-127.
16. Tempel, B.L., Papazian, D.M., Schwarz, T.L., Jan, Y.N., and Jan, L.Y. (1987). Sequence of a probable potassium channel component encoded at *Shaker* locus of drosophila. *Science* 237, 770-775.

17. Kaplan, W.D., and Trout, W.E. (1969). The behavior of four neurological mutants of *Drosophila*. *Genetics* 61, 399-409.
18. Salkoff, L., and Wyman, R. (1981). Genetic modification of potassium channels in *Drosophila* Shaker mutants. *Nature* 293, 228-230.
19. Papzian, D.M., Schwarz, T.L., Tempel, B.L., Jan, Y.N., and Jan, L.Y. (1987). Cloning of genomic and complementary DNA from shaker, a putative potassium channel gene from *Drosophila*. *Science* 237, 749-753.
20. Köhler, M., Hirschberg, B., Bond, C.T., Kinzie, J.M., Marrion, N.V., Maylie, J., and Adelman, J.P. (1996). Small-conductance, calcium-activated potassium channels from mammalian brain [see comments]. *Science* 273, 1709-1714.
21. Ishii, T.M., Silvia, C., Hirschberg, B., Bond, C.T., Adelman, J.P., and Maylie, J. (1997). A human intermediate conductance calcium-activated potassium channel. *Proc Natl Acad Sci USA* 94, 11651-11656.
22. Yu, F.H., Yarov-Yarovoy, V., Gutman, G.A., and Catterall, W.A. (2005). Overview of molecular relationships in the voltage-gated ion channel superfamily. *Pharmacol Rev* 57, 387-395.
23. Miller, C. (2000). An overview of the potassium channel family. *Genome Biol* 1, REVIEWS0004.
24. Ketchum, K.A., Jolner, W.J., Sellers, A.J., Kaczmarek, L.K., and Goldstein, S.A.N. (1995). A new family of outwardly rectifying potassium channel proteins with two pore domains in tandem. *Nature* 376, 690-695.
25. Goldstein, S.A., Price, L.A., Rosenthal, D.N., and Pausch, M.H. (1996). ORK1, a potassium-selective leak channel with two pore domains cloned from

- Drosophila melanogaster* by expression in *Saccharomyces cerevisiae*. *Proc Natl Acad Sci USA* 93, 13256-13261.
26. Katz, B. (1949). Les constantes electriques de la membrane du muscle. *Arch Sci Physiol* 2, 285-289.
27. Nichols, C.G., and Lopatin, A.N. (1997). Inward rectifier potassium channels. *Annual review of physiology* 59, 171-191.
28. Huang, C., Feng, S., and Hilgemann, D.W. (1998). Direct activation of inward rectifier potassium channels by PIP₂ and its stabilization by Gβγ. *Nature* 391, 803-806.
29. Ho, K., Nichols, C.G., Lederer, W.J., Lytton, J., Vassilev, P.M., Kanazirska, M.V., and Hebert, S.C. (1993). Cloning and expression of an inwardly rectifying ATP-regulated potassium channel. *Nature* 362, 31-37.
30. Lu, Z. (2004). Mechanism of rectification in inward-rectifier K⁺ channels. *Annual review of physiology* 66, 103-129.
31. Bichet, D., Haass, F.A., and Jan, L.Y. (2003). Merging functional studies with structures of inward-rectifier K(+) channels. *Nat Rev Neurosci* 4, 957-967.
32. Sigworth, F.J. (1994). Voltage gating of ion channels. *Quarterly reviews of biophysics* 27, 1-40.
33. Bezanilla, F. (2000). The voltage sensor in voltage-dependent ion channels. *Physiological reviews* 80, 555-592.
34. Jiang, Y., Ruta, V., Chen, J., Lee, A., and MacKinnon, R. (2003). The principle of gating charge movement in a voltage-dependent K⁺ channel. *Nature* 423, 42-48.

35. Palen, D.I., Belmadani, S., Lucchesi, P.A., and Matrougui, K. (2005). Role of SHP-1, Kv.1.2, and cGMP in nitric oxide-induced ERK1/2 MAP kinase dephosphorylation in rat vascular smooth muscle cells. *Cardiovascular research* 68, 268-277.
36. Gonzalez, C., Rosenman, E., Bezanilla, F., Alvarez, O., and Latorre, R. (2000). Modulation of the Shaker K(+) channel gating kinetics by the S3-S4 linker. *The Journal of general physiology* 115, 193-208.
37. Roeper, J., Lorra, C., and Pongs, O. (1997). Frequency-dependent inactivation of mammalian A-type K⁺ channel KV1.4 regulated by Ca²⁺/calmodulin-dependent protein kinase. *J Neurosci* 17, 3379-3391.
38. Wei, A.D., Gutman, G.A., Aldrich, R., Chandy, K.G., Grissmer, S., and Wulff, H. (2005). International Union of Pharmacology. LII. Nomenclature and molecular relationships of calcium-activated potassium channels. *Pharmacol Rev* 57, 463-472.
39. Schreiber, M., and Salkoff, L. (1997). A novel calcium-sensing domain in the BK channel. *Biophys J* 73, 1355-1363.
40. Xia, X.M., Zeng, X., and Lingle, C.J. (2002). Multiple regulatory sites in large-conductance calcium-activated potassium channels. *Nature* 418, 880-884.
41. Shi, J., Krishnamoorthy, G., Yang, Y., Hu, L., Chaturvedi, N., Harilal, D., Qin, J., and Cui, J. (2002). Mechanism of magnesium activation of calcium-activated potassium channels. *Nature* 418, 876-880.
42. Wilson, V.G., and Rosas-Acosta, G. (2005). Wrestling with SUMO in a new arena. *Sci STKE* 2005, pe32.

43. Gutman, G.A., Chandy, K.G., Grissmer, S., Lazdunski, M., McKinnon, D., Pardo, L.A., Robertson, G.A., Rudy, B., Sanguinetti, M.C., Stuhmer, W., *et al.* (2005). International Union of Pharmacology. LIII. Nomenclature and molecular relationships of voltage-gated potassium channels. *Pharmacol Rev* 57, 473-508.
44. Napp, J., Monje, F., Stuhmer, W., and Pardo, L.A. (2005). Glycosylation of Eag1 (Kv10.1) potassium channels: intracellular trafficking and functional consequences. *J Biol Chem* 280, 29506-29512.
45. Blaine, J.T., and Ribera, A.B. (1998). Heteromultimeric potassium channels formed by members of the Kv2 subfamily. *J Neurosci* 18, 9585-9593.
46. Shen, N.V., and Pfaffinger, P.J. (1995). Molecular recognition and assembly sequences involved in the subfamily-specific assembly of voltage-gated K⁺ channel subunit proteins. *Neuron* 14, 625-633.
47. Phartiyal, P., Jones, E.M., and Robertson, G.A. (2007). Heteromeric assembly of hERG 1A/1B channels occurs cotranslationally via amino-terminal interactions. *J Biol Chem*.
48. Li, Y., Um, S.Y., and McDonald, T.V. (2006). Voltage-gated potassium channels: regulation by accessory subunits. *Neuroscientist* 12, 199-210.
49. Cai, S.Q., Park, K.H., and Sesti, F. (2006). An evolutionarily conserved family of accessory subunits of K⁺ channels. *Cell biochemistry and biophysics* 46, 91-99.
50. Jenkinson, D.H. (2006). Potassium channels--multiplicity and challenges. *British journal of pharmacology* 147 Suppl 1, S63-71.

51. Isacoff, E.Y., Jan, Y.N., and Jan, L.Y. (1990). Evidence for the formation of heteromultimeric potassium channels in *Xenopus* oocytes. *Nature* 345, 530-534.
52. MacKinnon, R. (1991). Determination of the subunit stoichiometry of a voltage-activated potassium channel. *Nature* 350, 232-235.
53. McCormack, K., Lin, L., Iverson, L.E., Tanouye, M.A., and Sigworth, F.J. (1992). Tandem linkage of Shaker K⁺ channel subunits does not ensure the stoichiometry of expressed channels. *Biophysical journal* 63, 1406-1411.
54. Zhou, Y., Morais-Cabral, J.H., Kaufman, A., and MacKinnon, R. (2001). Chemistry of ion coordination and hydration revealed by a K⁺ channel- Fab complex at 2.0 Å resolution. *Nature* 414, 43-48.
55. Jiang, Y., Pico, A., Cadene, M., Chait, B.T., and MacKinnon, R. (2001). Structure of the RCK domain from the E. coli K⁺ channel and demonstration of its presence in the human BK channel. *Neuron* 29, 593-601.
56. Kuo, A., Gulbis, J.M., Antcliff, J.F., Rahman, T., Lowe, E.D., Zimmer, J., Cuthbertson, J., Ashcroft, F.M., Ezaki, T., and Doyle, D.A. (2003). Crystal structure of the potassium channel KirBac1.1 in the closed state. *Science* 300, 1922-1926.
57. Long, S.B., Campbell, E.B., and MacKinnon, R. (2005). Crystal structure of a mammalian voltage-dependent Shaker family K⁺ channel. *Science* 309, 897-903.
58. Biggin, P.C., Roosild, T., and Choe, S. (2000). Potassium channel structure: domain by domain. *Current opinion in structural biology* 10, 456-461.
59. Wissmann, R., Bildl, W., Oliver, D., Beyermann, M., Kalbitzer, H.R., Bontrop, D., and Fakler, B. (2003). Solution structure and function of the "tandem

- inactivation domain" of the neuronal A-type potassium channel Kv1.4. *J Biol Chem* 278, 16142-16150.
60. Choe, S. (2002). Potassium channel structures. *Nat Rev Neurosci* 3, 115-121.
61. Yellen, G. (2002). The voltage-gated potassium channels and their relatives. *Nature* 419, 35-42.
62. Schumacher, M.A., Rivard, A.F., Bachinger, H.P., and Adelman, J.P. (2001). Structure of the gating domain of a Ca²⁺-activated K⁺ channel complexed with Ca²⁺/calmodulin. *Nature* 410, 1120-1124.
63. Blatz, A.L., and Magleby, K.L. (1986). Single apamin-blocked Ca-activated K⁺ channels of small conductance in cultured rat skeletal muscle. *Nature* 323, 718-720.
64. Joiner, W.J., Wang, L.-Y., Tang, M.D., and Kaczmarek, L.K. (1997). hSK4, a member of a novel subfamily of calcium-activated potassium channels. *PNAS* 94, 11013-11018.
65. Xia, X.-M., Fakler, B., Rivard, A., Wayman, G., Johnson-Pais, T., Keen, J.E., Ishii, T., Hirschberg, B., Bond, C.T., Lutsenko, S., *et al.* (1998). Mechanism of calcium gating in small-conductance calcium-activated potassium channels. *Nature* 395, 503-507.
66. Keen, J.E., Khawaled, R., Farrens, D.L., Neelands, T., Rivard, A., Bond, C.T., Janowsky, A., Fakler, B., Adelman, J.P., and Maylie, J. (1999). Domains responsible for constitutive and Ca(2+)-dependent interactions between

- calmodulin and small conductance Ca(2+)-activated potassium channels. *J Neurosci* 19, 8830-8838.
67. Hirschberg, B., Maylie, J., Adelman, J.P., and Marrion, N.V. (1998). Gating of recombinant small conductance Ca-activated K⁺ channels by calcium. *J Gen Physiol* 111, 565-581.
68. Ishii, T.M., Maylie, J., and Adelman, J.P. (1997). Determinants of apamin and d-tubocurarine block in SK potassium channels. *J Biol Chem* 272, 23195-23200.
69. Shah, M., and Haylett, D.G. (2000). The pharmacology of hSK1 Ca²⁺-activated K⁺ channels expressed in mammalian cell lines. *British journal of pharmacology* 129, 627-630.
70. Strobaek, D., Jorgensen, T.D., Christophersen, P., Ahring, P.K., and Olesen, S.P. (2000). Pharmacological characterization of small-conductance Ca(2+)-activated K(+) channels stably expressed in HEK 293 cells. *British journal of pharmacology* 129, 991-999.
71. D'Hoedt, D., Hirzel, K., Pedarzani, P., and Stocker, M. (2004). Domain analysis of the calcium-activated potassium channel SK1 from rat brain. Functional expression and toxin sensitivity. *J Biol Chem* 279, 12088-12092.
72. Saimi, Y., and Kung, C. (2002). Calmodulin as an ion channel subunit. *Annual review of physiology* 64, 289-311.
73. Saimi, Y., and Ling, K.Y. (1990). Calmodulin activation of calcium-dependent sodium channels in excised membrane patches of *Paramecium*. *Science* 249, 1441-1444.

74. Hinrichsen, R.D., Burgess-Cassler, A., Soltvedt, B.C., Hennessey, T., and Kung, C. (1986). Restoration by calmodulin of a Ca^{2+} -dependent K^+ current missing in a mutant of *paramecium*. *Science* 232, 503-506.
75. Kink, J.A., Maley, M.E., Preston, R.R., Ling, K.-Y., Wallen-Friedman, M.A., Saimi, Y., and Kung, C. (1990). Mutations in *paramecium* calmodulin indicate functional differences between the C-terminal and N-terminal lobes *in vivo*. *Cell* 62, 165-174.
76. Saimi, Y., Hinrichsen, R.D., Forte, M., and Kung, C. (1983). Mutant analysis shows that the Ca^{2+} -induced K^+ current shuts off one type of excitation in *paramecium*. *Proc Natl Acad Sci, USA* 80, 5112-5116.
77. Lee, W.S., Ngo-Anh, T.J., Bruening-Wright, A., Maylie, J., and Adelman, J.P. (2003). Small Conductance Ca^{2+} -activated K^+ Channels and Calmodulin: Cell surface expression and gating. *J Biol Chem* 278, 25940-25946.
78. Meech, R.W. (1972). Intracellular calcium injection causes increased potassium conductance in *Aplysia* nerve cells. *Comparative biochemistry and physiology* 42, 493-499.
79. Krnjevic, K., and Lisiewicz, A. (1972). Injections of calcium ions into spinal motoneurons. *The Journal of physiology* 225, 363-390.
80. Schwartzkroin, A., and Stafstrom, C.E. (1980). Effects of EGTA on the calcium-activated afterhyperpolarization in the hippocampal CA3 pyramidal cells. *Science* 210, 1125-1126.
81. Hotson, J.R., and Prince, D.A. (1980). A calcium-activated hyperpolarization follows repetitive firing in hippocampal neurons. *J Neurophysiol* 43, 409-419.

82. Alger, B.E., and Nicoll, R.A. (1980). Epileptiform burst after hyperpolarization: calcium-dependent potassium potential in hippocampal CA1 pyramidal cells. *Science* 210, 1122-1124.
83. Burgess, G.M., Claret, M., and Jenkinson, D.H. (1981). Effects of quinine and apamin on the calcium-dependent potassium permeability of mammalian hepatocytes and red cells. *The Journal of physiology* 317, 67-90.
84. Dimpfel, W., Pierau, F.K., and Haider, S.G. (1979). Electrophysiological studies on the effects of the neurotoxin apamin on cultured neurons. *Advances in cytopharmacology* 3, 395-399.
85. Banks, B.E.C., Brown, C., Burgess, G.M., Burnstock, G., Claret, M., Cocks, T.M., and Jenkinson, D.H. (1979). Apamin blocks certain neurotransmitter-induced increases in potassium permeability. *Nature* 282, 415-417.
86. Blatz, A.L., and Magleby, K.L. (1987). Calcium-activated potassium channels. *Trends Neurosci* 10, 463-467.
87. Pribnow, D., Johnson-Pais, T., Bond, C.T., Keen, J., Johnson, R.A., Janowsky, A., Silvia, C., Thayer, M., Maylie, J., and Adelman, J.P. (1999). Skeletal muscle and small-conductance calcium-activated potassium channels. *Muscle Nerve* 22, 742-750.
88. Neelands, T.R., Herson, P.S., Jacobson, D., Adelman, J.P., and Maylie, J. (2001). Small-conductance calcium-activated potassium currents in mouse hyperexcitable denervated skeletal muscle. *The Journal of physiology* 536, 397-407.

89. Jacobson, D., Herson, P.S., Neelands, T.R., Maylie, J., and Adelman, J.P. (2002). SK channels are necessary but not sufficient for denervation-induced hyperexcitability. *Muscle Nerve* 26, 817-822.
90. Kimura, T., Takahashi, M.P., Okuda, Y., Kaido, M., Fujimura, H., Yanagihara, T., and Sakoda, S. (2000). The expression of ion channel mRNAs in skeletal muscles from patients with myotonic muscular dystrophy. *Neurosci Lett* 295, 93-96.
91. Vincent, J.-P., Schweitz, H., and Lazdunski, M. (1975). Structure-function relationships and site of action of apamin, a neurotoxic polypeptide of bee venom with an action on the central nervous system. *J Biochem* 14, 2521.
92. Hugues, M., Romey, G., Duval, D., Vincent, J.P., and Lazdunski, M. (1982). Apamin as a selective blocker of the calcium-dependent potassium channel in neuroblastoma cells: voltage-clamp and biochemical characterization of the toxin receptor. *Proc Natl Acad Sci USA* 79, 1308-1312.
93. Hugues, M., Schmid, H., Romey, G., duval, D., Frelin, C., and Lazdunski, M. (1982). The Ca²⁺-dependent slow K⁺ conductance in cultured rat muscle cells: characterization with apamin. *EMBO* 9, 1039-1042.
94. Lazdunski, M. (1983). Apamin, a neurotoxin specific for one class of Ca²⁺-dependent K⁺ channels. *Cell calcium* 4, 421-428.
95. Sailer, C.A., Kaufmann, W.A., Marksteiner, J., and Knaus, H.G. (2004). Comparative immunohistochemical distribution of three small-conductance Ca²⁺-activated potassium channel subunits, SK1, SK2, and SK3 in mouse brain. *Mol Cell Neurosci* 26, 458-469.

96. Abel, H.J., Lee, J.C., Callaway, J.C., and Foehring, R.C. (2004). Relationships between intracellular calcium and afterhyperpolarizations in neocortical pyramidal neurons. *Journal of neurophysiology* 91, 324-335.
97. Sah, P. (1996). Ca^{2+} - activated K^{+} currents in neurones: types, physiological roles and modulation. *Trends Neurosci* 19, 150-154.
98. Ngo-Anh, T.J., Bloodgood, B.L., Lin, M., Sabatini, B.L., Maylie, J., and Adelman, J.P. (2005). SK channels and NMDA receptors form a Ca^{2+} -mediated feedback loop in dendritic spines. *Nature neuroscience* 8, 642-649.
99. Cai, X., Liang, C.W., Muralidharan, S., Kao, J.P., Tang, C.M., and Thompson, S.M. (2004). Unique roles of SK and Kv4.2 potassium channels in dendritic integration. *Neuron* 44, 351-364.
100. Tsai, S.Y., Tsai, M.-J., and O'Malley, B.W. (1989). Cooperative Binding of Steroid Hormone Receptors Contributes to Transcriptional Synergism at Target Enhancer Elements. *Cell* 57, 443-448.
101. Hille, B. (1992). *Ionic Channels of Excitable Membranes* (Sunderland, Sinauer Associates Inc.).
102. Erickson, K.R., Ronnekliev, O.K., and Kelly, M.J. (1993). Electrophysiology of guinea-pig supraoptic neurones: role of hyperpolarization-activated cation current in phasic firing. *J Physiol* 460, 407-425.
103. Erickson, K.R., Ronnekliev, O.K., and Kelly, M.J. (1993). Role of a T-type calcium current in supporting a depolarizing potential, damped oscillations, and phasic firing in vasopressinergic guinea pig supraoptic neurons. *Neuroendocrinology* 57, 789-800.

104. Taylor, M.S., Bonev, A.D., Gross, T.P., Eckman, D.M., Brayden, J.E., Bond, C.T., Adelman, J.P., and Nelson, M.T. (2003). Altered expression of small-conductance Ca²⁺-activated K⁺ (SK3) channels modulates arterial tone and blood pressure. *Circ Res* 93, 124-131.
105. Herrera, G.M., Pozo, M.J., Zvara, P., Petkov, G.V., Bond, C.T., Adelman, J.P., and Nelson, M.T. (2003). Urinary bladder instability induced by selective suppression of the murine small conductance calcium-activated potassium (SK3) channel. *The Journal of physiology* 551, 893-903.
106. Devor, D.C., Singh, A.K., Gerlach, A.C., Frizzell, R.A., and Bridges, R.J. (1997). Inhibition of intestinal Cl⁻ secretion by clotrimazole: direct effect on basolateral membrane K⁺ channels. *The American journal of physiology* 273, C531-540.
107. Begenisich, T., Nakamoto, T., Ovitt, C.E., Nehrke, K., Brugnara, C., Alper, S.L., and Melvin, J.E. (2004). Physiological roles of the intermediate conductance, Ca²⁺-activated potassium channel Kcnn4. *J Biol Chem* 279, 47681-47687.
108. Bond, C.T., Herson, P.S., Strassmaier, T., Hammond, R., Stackman, R., Maylie, J., and Adelman, J.P. (2004). Small conductance Ca²⁺-activated K⁺ channel knock-out mice reveal the identity of calcium-dependent afterhyperpolarization currents. *J Neurosci* 24, 5301-5306.
109. Bond, C.T., Sprengel, R., Bissonnette, J.M., Kaufmann, W.A., Pribnow, D., Neelands, T., Storck, T., Baetscher, M., Jerecic, J., Maylie, J., *et al.* (2000).

Respiration and parturition affected by conditional overexpression of the Ca²⁺-activated K⁺ channel subunit, SK3. *Science* 289, 1942-1946.

110. Singh, S., and Wu, C.F. (1999). Ionic currents in larval muscles of *Drosophila*. *Int Rev Neurobiol* 43, 191-220.

111. Wicher, D., Walther, C., and Wicher, C. (2001). Non-synaptic ion channels in insects--basic properties of currents and their modulation in neurons and skeletal muscles. *Prog Neurobiol* 64, 431-525.

112. Covarrubias, M., Wei, A., and Salkoff, L. (1991). *Shaker*, *Shal*, *Shab*, and *Shaw* express independent K⁺ current systems. *Neuron* 7, 763-773.

113. Ganetzky, B., and Wu, C.F. (1982). *Drosophila* mutants with opposing effects on nerve excitability: genetic and spatial interactions in repetitive firing. *Journal of neurophysiology* 47, 501-514.

114. Adelman, J.P., Shen, K.Z., Kavanaugh, M.P., Warren, R.A., Wu, Y.N., Lagrutta, A., Bond, C.T., and North, R.A. (1992). Calcium-activated potassium channels expressed from cloned complementary DNAs. *Neuron* 9, 209-216.

115. Tempel, B.L., Jan, Y.N., and Jan, L.Y. (1988). Cloning of a probable potassium channel gene from mouse brain. *Nature* 332, 837-839.

116. Frech, G.C., VanDongen, A.M.J., Schuster, G., Brown, A.M., and Joho, R.H. (1989). A novel potassium channel with delayed rectifier properties isolated from rat brain by expression cloning. *Nature* 340, 642-645.

117. Grissmer, S., Ghanshani, S., Dethlefs, B., McPherson, J.D., Wasmuth, J.J., Gutman, G.A., Cahalan, M.D., and Chandy, K.G. (1992). The Shaw-related

potassium channel gene, Kv3.1, on human chromosome 11, encodes the type I K⁺ channel in T cells. *J Biol Chem* 267, 20971-20979.

118. Pak, M.D., Baker, K., Covarrubias, M., Butler, A., Ratcliffe, A., and Salkoff, L. (1991). mShal, a subfamily of A-type K⁺ channel cloned from mammalian brain. *Proc Natl Acad Sci U S A* 88, 4386-4390.

119. Wei, A., and Salkoff, L. (1986). Occult *Drosophila* calcium channels and twinning of calcium and voltage- activated potassium channels. *Science* 233, 780-782.

120. Celniker, S.E., Wheeler, D.A., Kronmiller, B., Carlson, J.W., Halpern, A., Patel, S., Adams, M., Champe, M., Dugan, S.P., Frise, E., *et al.* (2002). Finishing a whole-genome shotgun: release 3 of the *Drosophila melanogaster* euchromatic genome sequence. *Genome Biol* 3, RESEARCH0079.

121. Bellen, H.J., Levis, R.W., Liao, G., He, Y., Carlson, J.W., Tsang, G., Evans-Holm, M., Hiesinger, P.R., Schulze, K.L., Rubin, G.M., *et al.* (2004). The BDGP gene disruption project: single transposon insertions associated with 40% of *Drosophila* genes. *Genetics* 167, 761-781.

122. Roberts, D.B., ed. (1998). *Drosophila A Practical Approach*, second edition (Oxford, Oxford University Press).

123. Rozen, S., and Skaletsky, H. (2000). Primer3 on the WWW for general users and for biologist programmers. *Methods Mol Biol* 132, 365-386.

124. Vo, N., Klein, M.E., Varlamova, O., Keller, D.M., Yamamoto, T., Goodman, R.H., and Impey, S. (2005). A cAMP-response element binding protein-induced

microRNA regulates neuronal morphogenesis. *Proc Natl Acad Sci U S A* 102, 16426-16431.

125. Livak, K.J. (1997). ABI Prism 7700 Sequence Detection System User Bulletin #2 (PE Applied Biosystems), pp. 1-36.

126. Jan, L.Y., and Jan, Y.N. (1976). Properties of the larval neuromuscular junction in *Drosophila melanogaster*. *The Journal of physiology* 262, 189-214.

127. Chenna, R., Sugawara, H., Koike, T., Lopez, R., Gibson, T.J., Higgins, D.G., and Thompson, J.D. (2003). Multiple sequence alignment with the Clustal series of programs. *Nucleic acids research* 31, 3497-3500.

128. Spradling, A.C., Stern, D.M., Kiss, I., Roote, J., Lavery, T., and Rubin, G.M. (1995). Gene disruptions using P transposable elements: an integral component of the *Drosophila* genome project. *Proc Natl Acad Sci U S A* 92, 10824-10830.

129. Sharma, Y., Cheung, U., Larsen, E.W., and Eberl, D.F. (2002). PPTGAL, a convenient Gal4 P-element vector for testing expression of enhancer fragments in *drosophila*. *Genesis* 34, 115-118.

130. Duffy, J.B. (2002). GAL4 system in *Drosophila*: a fly geneticist's Swiss army knife. *Genesis* 34, 1-15.

131. Brand, A.H., and Perrimon, N. (1993). Targeted gene expression as a means of altering cell fates and generating dominant phenotypes. *Development* 118, 401-415.

132. Harrison, D.A., Binari, R., Nahreini, T.S., Gilman, M., and Perrimon, N. (1995). Activation of a *Drosophila* Janus kinase (JAK) causes hematopoietic neoplasia and developmental defects. *Embo J* 14, 2857-2865.

133. Luo, L., Liao, Y.J., Jan, L.Y., and Jan, Y.N. (1994). Distinct morphogenetic functions of similar small GTPases: *Drosophila* Drac1 is involved in axonal outgrowth and myoblast fusion. *Genes & development* 8, 1787-1802.
134. Rong, Y.S., and Golic, K.G. (2000). Gene targeting by homologous recombination in *Drosophila*. *Science* 288, 2013-2018.
135. Balter, H., Griffith, C.S., and Margulies, L. (1992). Radiation and transposon-induced genetic damage in *Drosophila melanogaster*: X-ray dose-response and synergism with DNA-repair deficiency. *Mutat Res* 267, 31-42.
136. Huet, F., Lu, J.T., Myrick, K.V., Baugh, L.R., Crosby, M.A., and Gelbart, W.M. (2002). A deletion-generator compound element allows deletion saturation analysis for genomewide phenotypic annotation. *Proc Natl Acad Sci U S A* 99, 9948-9953.
137. Brenner, R., Yu, J.Y., Srinivasan, K., Brewer, L., Larimer, J.L., Wilbur, J.L., and Atkinson, N.S. (2000). Complementation of physiological and behavioral defects by a slowpoke Ca(2+) -activated K(+) channel transgene. *J Neurochem* 75, 1310-1319.
138. Siddiqi, O., Benzer, S. (1976). Neurological defects in temperature-sensitive paralytic mutants of *Drosophila melanogaster*. *Proc Natl Acad Sci USA* 73, 3253-3257.
139. Jaramillo, A.M., Zheng, X., Zhou, Y., Amado, D.A., Sheldon, A., Sehgal, A., and Levitan, I.B. (2004). Pattern of distribution and cycling of SLOB, Slowpoke channel binding protein, in *Drosophila*. *BMC Neurosci* 5, 3.

140. Elkins, T., Ganetzky, B., and Wu, C.-F. (1986). A *Drosophila* mutation that eliminates a calcium-dependent potassium current. *Proc Nat Acad Sci USA* 83, 8415-8419.
141. Butler, A., Wei, A., Baker, K., and Salkoff, L. (1989). A family of putative potassium channel genes in drosophila. *Science* 243, 943-947.
142. Hegde, P., Gu, G.G., Chen, D., Free, S.J., and Singh, S. (1999). Mutational analysis of the Shab-encoded delayed rectifier K(+) channels in *Drosophila*. *J Biol Chem* 274, 22109-22113.
143. Wolfart, J., Neuhoff, H., Franz, O., and Roeper, J. (2001). Differential expression of the small-conductance, calcium-activated potassium channel SK3 is critical for pacemaker control in dopaminergic midbrain neurons. *J Neurosci* 21, 3443-3456.
144. Blank, T., Nijholt, I., Kye, M.J., Radulovic, J., and Spiess, J. (2003). Small-conductance, Ca²⁺-activated K⁺ channel SK3 generates age-related memory and LTP deficits. *Nature neuroscience* 6, 911-912.
145. Takahata, T., Hayashi, M., and Ishikawa, T. (2003). SK4/IK1-like channels mediate TEA-insensitive, Ca²⁺-activated K⁺ currents in bovine parotid acinar cells. *American journal of physiology* 284, C127-144.
146. Thompson, J., and Begenisich, T. (2006). Membrane-delimited inhibition of maxi-K channel activity by the intermediate conductance Ca²⁺-activated K channel. *The Journal of general physiology* 127, 159-169.
147. Si, H., Heyken, W.T., Wolfle, S.E., Tysiac, M., Schubert, R., Grgic, I., Vilianovich, L., Giebing, G., Maier, T., Gross, V., *et al.* (2006). Impaired

endothelium-derived hyperpolarizing factor-mediated dilations and increased blood pressure in mice deficient of the intermediate-conductance Ca²⁺-activated K⁺ channel. *Circ Res* 99, 537-544.

148. Rubin, G.M., and Lewis, E.B. (2000). A brief history of *Drosophila*'s contributions to genome research. *Science* 287, 2216-2218.

149. Nusslein-Volhard, C., and Wieschaus, E. (1980). Mutations affecting segment number and polarity in *Drosophila*. *Nature* 287, 795-801.

150. Homyk, T., Jr., Szidonya, J., and Suzuki, D.T. (1980). Behavioral mutants of *Drosophila melanogaster*. III. Isolation and mapping of mutations by direct visual observations of behavioral phenotypes. *Mol Gen Genet* 177, 553-565.

151. Adams, M.D., and Sekelsky, J.J. (2002). From sequence to phenotype: reverse genetics in *Drosophila melanogaster*. *Nat Rev Genet* 3, 189-198.

152. Spradling, A.C., Stern, D., Beaton, A., Rhem, E.J., Lavery, T., Mozden, N., Misra, S., and Rubin, G.M. (1999). The Berkeley *Drosophila* Genome Project gene disruption project: Single P-element insertions mutating 25% of vital *Drosophila* genes. *Genetics* 153, 135-177.

153. Cutler, S., and McCourt, P. (2005). Dude, where's my phenotype? Dealing with redundancy in signaling networks. *Plant physiology* 138, 558-559.

154. Seecof, R.L., Alleaume, N., Teplitz, R.L., and Gerson, I. (1971). Differentiation of neurons and myocytes in cell cultures made from *Drosophila* gastrulae. *Experimental cell research* 69, 161-173.

155. Wu, C.-F., and Haugland, F.N. (1985). Voltage clamp analysis of membrane currents in larval muscle fibers of *Drosophila*: alteration of potassium currents in *Shaker* mutants. *J Neuroscience* 5, 2626-2640.
156. Salkoff, L., and Wyman, R. (1981). Outward currents in developing *Drosophila* flight muscle. *Science* 212, 461-463.
157. Wu, C.F., Ganetzky, B., Jan, L.Y., and Jan, Y.N. (1978). A *Drosophila* mutant with a temperature-sensitive block in nerve conduction. *Proc Natl Acad Sci U S A* 75, 4047-4051.
158. Ueda, A., and Wu, C.F. (2006). Distinct frequency-dependent regulation of nerve terminal excitability and synaptic transmission by IA and IK potassium channels revealed by *Drosophila* *Shaker* and *Shab* mutations. *J Neurosci* 26, 6238-6248.
159. Peng, I.F., and Wu, C.F. (2007). Differential contributions of *Shaker* and *Shab* K⁺ currents to neuronal firing patterns in *Drosophila*. *Journal of neurophysiology* 97, 780-794.
160. Wu, C.F., and Ganetzky, B. (1992). Neurogenetic studies of ion channels in *Drosophila*. *Ion channels* 3, 261-314.
161. Littleton, J.T., and Ganetzky, B. (2000). Ion channels and synaptic organization: analysis of the *Drosophila* genome. *Neuron* 26, 35-43.
162. Gerlach, A.C., Maylie, J., and Adelman, J.P. (2004). Activation kinetics of the slow afterhyperpolarization in hippocampal CA1 neurons. *Pflugers Arch*.
163. Torres, C.E., Chaput, Y., and Andrade, R. (1995). Cyclic AMP and protein kinase A mediate 5-hydroxytryptamine type 4 receptor regulation of calcium-

activated potassium current in adult hippocampal neurons. *Mol Pharmacol* 47, 191-197.

164. Delgado, R., Hidalgo, P., Diaz, F., Latorre, R., and Labarca, P. (1991). A cyclic AMP-activated K⁺ channel in *Drosophila* larval muscle is persistently activated in *dunce*. *Proc Natl Acad Sci USA* 88, 557-560.

165. Zhong, Y., and Wu, C.F. (1993). Differential modulation of potassium currents by cAMP and its long-term and short-term effects: *dunce* and *rutabaga* mutants of *Drosophila*. *J Neurogenet* 9, 15-27.

166. Wang, J.W., Humphreys, J.M., Phillips, J.P., Hilliker, A.J., and Wu, C.F. (2000). A novel leg-shaking *Drosophila* mutant defective in a voltage-gated K(+)current and hypersensitive to reactive oxygen species. *J Neurosci* 20, 5958-5964.

167. Lancaster, B., and Adams, P.R. (1986). Calcium-dependent current generating the afterhyperpolarization of hippocampal neurons. *Journal of neurophysiology* 55, 1268-1282.

168. Brakefield, P.M., and French, V. (2005). Evolutionary developmental biology: how and why to spot fly wings. *Nature* 433, 466-467.

169. Warmke, J., Drysdale, R., and Ganetzky, B. (1991). A distinct potassium channel polypeptide encoded by the *drosophila eag* locus. *Science* 252, 1560-1564.

170. Zhong, Y., and Wu, C.-F. (1991). Alteration of four identified K⁺ currents in *drosophila* muscle by mutations in *eag*. *Science* 252, 1562-1564.

171. Mayer, R.J., and Brown, I.R. (1994). Heat shock proteins in the nervous system (London ; San Diego, Academic Press).
172. Stapleton, M., Carlson, J.W., and Celniker, S.E. (2006). RNA editing in *Drosophila melanogaster*: New targets and functional consequences. *RNA* (New York, NY) 12, 1922-1932.
173. Zhang, Z., and Carmichael, G.G. (2001). The fate of dsRNA in the nucleus: a p54(nrb)-containing complex mediates the nuclear retention of promiscuously A-to-I edited RNAs. *Cell* 106, 465-475.
174. Das, A.K., and Carmichael, G.G. (2005). Unleash the messenger. *Nature cell biology* 7, 1054-1055.
175. Prasanth, K.V., Prasanth, S.G., Xuan, Z., Hearn, S., Freier, S.M., Bennett, C.F., Zhang, M.Q., and Spector, D.L. (2005). Regulating gene expression through RNA nuclear retention. *Cell* 123, 249-263.
176. Sommer, B., Kohler, M., Sprengel, R., and Seeburg, P.H. (1991). RNA editing in brain controls a determinant of ion flow in glutamate-gated channels. *Cell* 67, 11-19.
177. Burns, C.M., Chu, H., Rueter, S.M., Hutchinson, L.K., Canton, H., Sanders-Bush, E., and Emeson, R.B. (1997). Regulation of serotonin-2C receptor G-protein coupling by RNA editing. *Nature* 387, 303-308.
178. Palladino, M.J., Keegan, L.P., O'Connell, M.A., and Reenan, R.A. (2000). A-to-I pre-mRNA editing in *Drosophila* is primarily involved in adult nervous system function and integrity. *Cell* 102, 437-449.

179. Palladino, M.J., Keegan, L.P., O'Connell, M.A., and Reenan, R.A. (2000). dADAR, a *Drosophila* double-stranded RNA-specific adenosine deaminase is highly developmentally regulated and is itself a target for RNA editing. *RNA* (New York, NY) 6, 1004-1018.
180. Ma, E., Gu, X.Q., Wu, X., Xu, T., and Haddad, G.G. (2001). Mutation in pre-mRNA adenosine deaminase markedly attenuates neuronal tolerance to O₂ deprivation in *Drosophila melanogaster*. *The Journal of clinical investigation* 107, 685-693.
181. Haddad, G.G., Wyman, R.J., Mohsenin, A., Sun, Y., and Krishnan, S.N. (1997). Behavioral and Electrophysiologic Responses of *Drosophila melanogaster* to Prolonged Periods of Anoxia. *J Insect Physiol* 43, 203-210.
182. Haddad, G.G. (2006). Tolerance to low O₂: lessons from invertebrate genetic models. *Experimental physiology* 91, 277-282.
183. Keating, D.J., Rychkov, G.Y., Giacomini, P., and Roberts, M.L. (2005). Oxygen-sensing pathway for SK channels in the ovine adrenal medulla. *Clinical and experimental pharmacology & physiology* 32, 882-887.
184. Lee, J., Lim, W., Eun, S.Y., Kim, S.J., and Kim, J. (2000). Inhibition of apamin-sensitive K⁺ current by hypoxia in adult rat adrenal chromaffin cells. *Pflugers Arch* 439, 700-704.
185. Quesada, I., and Verdugo, P. (2005). InsP₃ signaling induces pulse-modulated Ca²⁺ signals in the nucleus of airway epithelial ciliated cells. *Biophysical journal* 88, 3946-3953.

186. Stockwell, B.R. (2000). Chemical genetics: ligand-based discovery of gene function. *Nat Rev Genet* 1, 116-125.

Appendix

Item A) Mutant lines dSK3.2 and dSK7.2 were, strictly speaking, transpositions. 44kb of the SK gene sequence was replaced with 2.7kb of sequence homologous to the *hobo* transposase. The inserted *hobo* sequence in both null lines was identical and is given below.

```
GAGAACTGCAGCCCGCCACTCGCACTCTACGTCCACCCGATAAACACTCGGTACTCTAG
GCACCCCGTTTTTTTTGACACCCTACTTGCGGCAACACAAAATACTCGAGTGTTTTACC
GACGTTGTGTTTTGTTACGAGTAAAAAACACCCGAGGCCTGCTGCGCAAGAGCCGT
ATGGGTGAGTGGACGCACAGTCAACGATCGGCCGAGGTCATTTTTTGTATGCGGGCTG
CAGTTCTCATTTTTGTACGCCATAAATTTGTATGGGTGGAAGCGTGACGGGTATAAGA
AATGAAGGGTAAAAGGGAATACCCAAGAAAATTTTTGTGCTCATGTCTTTGCTCTTTGA
TGGACTCAATGGGTGCCTCCCATTTCAAACACATAAAGTAATTGCAATTAAAGACGGCA
TTTGTGATTTTTACGTTTTTTAATGTCTCAATCTAAATAATAAAAACATAGTGGGCTT
AAAAAGTATCTATTAAATATAAGGAACCTTACTTTTACATTTTTTAGGATTTTGCAT
CTAATGTCTTAACAAATAACAATCTTATATATTATTAATTAATACTTATACTTAATACT
TAACACTTATACAAAATTAAGCAAATAATAAGAATTAATAATATAAAATATACTTATA
AGAAGGAATATCTATTGCGAGTTGTTTAGGTTTTGTAAATAGGAATGCAAAAAAGGAG
GCTATCTACAGATTTTGGGCATAATCTATTTTCGTTTTCTGTTATTATATTACCTGCTA
GGGAAACACTCTTTCAGCTGCTGCGCTACTGGCTGGTATTGATAAAAAGTTTTAATGCT
AACTTTGACAACCTGAGGGTATAAGTTTGCGTTATTTTTCCACCACTCAATTACTTCAA
ATTTTGAGACAATGGAACCTTTGTCTAATATATCGTTCAATTCATCTAATGGAGATT
CATTGAAGTTGGAATTAGACTCAGTTACTAACTTTGGGAAGAAGAATTCGTTTTCAGAA
GATATTGTTTTGTTTTTTTTTGGAAATAAGTTGGACTTTCTAGACTTTCTGGAGTTTCT
TGGAGTTTCTGGAGTTTCTGGAGTTTCTGGAGTTTCTGGAGTTTCTGGAGTTTCTGTAG
ATTCTAAGCTTAATGTGTATGAAATTGGGACTTGAATTTGTGAAATGCAAAACACCTTT
ATTTCAAGAATATCTTCTTCCCTGAAGATGTGCTGCGGGTGGATATAAAAAAATGCCGC
CTTATGCCATATGCTTAGATTTGCCATCCAAATCTTACGAATATTTTCCAAAATCTTT
CCTTAAGCAATGCTGCTGCAGAAAGGTCTAAAATATTCGGCTCGCATAATTCTAAAATT
TTAGAGATGGATGGCAATACGAAGCATATAGATGGTGAGCTAGATGTTTGCATTTGAGT
TCATTGGCCTCGTTAAACGATTTTTCTAAAACATTTGACAACAGGTGACTGCTACAATT
TAAACGGGTATTGCCCTCTAAAGCCTTTTTTATATTTGCTCCCCTGTCAGTCACAACT
TAACATTATCAATGTTCTCAACATTGAATTCGAAAATAAACCTTTAATTTTCATTA
ATGTTTTCGGCAGTCGATTTTTGAAAATTCATCGATTTTAGTCCCAAATCATGTCACA
AAGTTTAAATCTTTTTCGTAATGGAAAGTGATGCCCAAAAGTTTCTTTGGACATACT
GGTCAGTCCACATGTCGACGGTCGCACTTGCTCTTCCGCTATCCACAGCTTTTTTTATC
TCGGACGAGATTAGACTCCTCTTCTTCTGTCATCCGATTTGGCCTTCCGACTTAATGT
TGTTGGATCAGGTAGTAAGTCATCGACGTCTACCTGTTCCCATAGATAGCGCCGATTT
GTAGGAAAACCTTACCAAATTTTTAAATCCGGCTCCGGTACTGCAGAAAACGGCCGA
CAATCTTGGACAACCCATTGGGTGCATTTTTCAATAGCTACTTTCTTGTGCTTTTCCGA
ACAATTTTTAATTCGTTGGTCTTAAATGTTAGACAACATTTATGGCGGGATAAAT
TGGAGGTGTTTTGTGTAATAAATTTGAGCACTTTCTGGCATTGCCTGCAGAACAGCCAT
CCGTCCAGAACAGTTTCATCTTCTTTAAATGTACATAAAATGCTCCAAATAACACT
TTTCCCTTATGTTTATTGGCAACTGAGTATGTTCCATTGTTAATTTTATTTTAAACGA
```

AATCAGCCGCTTCTGCCATTATTGTGACCTTTTCCTTTGGCTTCCAAATAATACTGAAT
CCTAACAAGCTAGTAATTGCATCGTAAAAAACAAAAAGGGGCAATTAACAGCCGAGAC
ACTGGACCAAAGACACAAGAACTCAACAATCATTATGTATGGCGCCATTTGACTCGACT
ACCTACGAGACCACTCGAGTATTTTTGGAAACACCCGAGTATTTTTGGAAACACCCATG
TGTTTAAACGGTATACCCACAAGTGTTTTTCTCACTCATCCCTTTTTAGGCACTGTGTGA
GCGGCACCCGCGACGCAAAACACCGTATTGATTCGGGTGCGCACACAACGGGGTGTCTT
GTCTGCATGTTTCAGATTTATACTGTGTGTTTGTAAAGTACCCGCGATGTGCGTGGCGAGT
AGCACCCGACACAAAATTGTAGGGTGTGAGTCGAGTGGTAAAAAAGTGCCACCCTTGC
AGTTCTCTG

Item B) Sequence of the dSK/rSK2 chimera. The extracellular N- and C-termini of rSK2 (**bold**) flank the transmembrane core of dSK (normal typeface).

ATGAGCAGCTGCAGGTACAACGGGGGCGTCATGCGTCCGCTCAGCAACTTGAGCTCGTC
CCGCCGGAACCTGCACGAGATGGACTCAGAGGCTCAGCCCTGCAGCCCCAGCGTCGG
TTGTAGGAGGAGGTGGTGGTGCCTCCTCCCGTCTGCTGCCGCCGCCCTCATCCTCA
GCCCCAGAGATCGTGGTGTCTAAGCCGGAGCACAACAATTCTAACAACCTGGCGCTCTA
CGGAACTGGCGGCGGAGGCAGCACCGGAGGCGCGGCGGCGGCGGCGGCGGCGGCGG
GCAGCGGGCATGGCAGCAGCAGCGGCACTAAGTCCAGCAAAAAGAAGAACCAGAACATC
GGCTATAAGCTGGGAAAGAGGAAAGCCCTCTTCGAGAAGCGCAAACGGATCAGCGATTA
CGCCCTGGTCATGGGCATGTTCCGGGATCATCGTGATGGTTATCGAAAACGAACTGAGCA
GTGCCGGTGTCTACACAAAGGCATCGTTCCTACTCGACAGCGTTAAAAACCTTAATATCT
GTTTCGACTGTGATTCTTTTAGGACTTATAGTAGCTTACCATGCTTTGGAAGTGCAGTT
ATTCATGATAGATAACTGCGCTGACGATTGGAGGATCGCAATGACATGGCAACGAATTA
GTCAAATAGGGTTAGAACTTTTTATATGCGCTATACATCCAATTCCTGGCGAATACTAT
TTCCAGTGGACGACGAAATTTGGCCAATAAGAATAAAACAATTGGCACCGAAATGGTGCC
ATATGACGTAGCTTTATCATTACCTATGTTCCCTTCGATTATATTTAATCTGCCGCGTAA
TGCTGCTGCATTCAAAGCTATTCACAGATGCATCATCACGGAGCATTGGCGCTCTCAAT
AGGATTAATTTTAAACACAAGATTCGTTTTAAAACTCTAATGACAATATGTCCGGGAAC
GGTCTATTGGTCTTCATGGTCTCGCTGTGGATCATCGCATCGTGGACGCTGCGTCAGT
GCGAAAGGTTCCACGATGAGGAGCACGCGAATTTGCTAAACTCCATGTGGCTAACGGCC
ATCACATTTCTGTGTGTCGGCTACGGCGACATTGTGCCAAACACGTACTGTGGACGCGG
TATCACCTCACCTGCGGCATGGTGGGCGCCGGCTGTACGGCTCTACTGGTGGCCGTAG
TCTCTCGGAAACTGGAGCTGACCAAGCAGAAAAGCATGTGCACAATTCATGATGGAT
ACTCAGCTGACCAAAAGAGTAAAAACGCAGCCGCCAATGTACTCAGGGAAACGTGGTT
AATCTACAAAACACAAAGCTAGTGAAAAGATCGACCATGCAAAGTAAGGAAGCATC
AACGGAATTCCTTACAAGCTATTCATCAATTAAGAAGTGTGAAGATGGAACAGAGGAAA
CTGAATGACCAAGCGAATACTCTAGTGGATCTGGCAAAGACCCAGAATATCATGTATGA
TATGATTTCCGACTTAAATGAAAGGAGTGAAGACTTTGAGAAAAGGATCGTCACCCTGG
AAACAAAATTAGAACTTTGATTGGTAGCATTATGCCCTCCCTGGGCTTATCAGCCAG
ACCATCAGACAGCAGCAAAGGGACTTCATAGAGACACAGATGGAGAACTATGACAAGCA
TGTCACCTACAATGCTGAGCGTTCCTCGTCCAGGAGGCGGCGGTCCTCCTCCA

Item C) Nucleotide sequence of the two probes used for the Northern blots shown in Figure 8:

Probe for exons 3-6:

CCCAATGTGGGCTATCGCCTGGGAAAAGAGGAAAGCCCTCTTCGAGAAGCGCAAACGGAT
CAGCGATTACGCCCTGGTCATGGGCATGTTTCGGGATCATCGTGATGGTTATCGAAAACG
AACTGAGCAGTGCCGGTGTCTACACAAAGGCATCGTTCTACTCGACAGCGTTAAAAACC
TTAATATCTGTTTCGACTGTGATTCTTTTAGGACTTATAGTAGCTTACCATGCTTTGGA
AGTGCAGTTATTCATGATAGATAACTGCGCTGACGATTGGAGGATCGCAATGACATGGC
AACGAATTAGTCAAATAGGGTTAGAACTTTTTATATGCGCTATACATCCAATTCCTGGC
GAATACTATTTCCAGTGGACGACGAAATTGGCCAATAAGAATAAAACAATTGGCACCGA
AATGGTGCCATATGACGTAGCTTTATCATTACCTATGTTCCCTCGATTATATTTAATCT
GCCGCGTAATGCTGCTGCATTCAAAGCTATTCACAGATGCATCATCACGGAGCATTGGC
GCTCTCAATAGGATTAATTTTAAACACAAGATTCGTTTTAAAACTCTAATGACAATATG
TCCGGGAACGGTTCTATTGGTCTTCATGGTCTCG

Probe for exons 8-13:

GGCTGTACGGCTCTACTGGTGGCCGTAGTCTCTCGGAAACTGGAGCTGACCCGTGCTGA
GAAGCATGTGCACAACCTTCATGATGGACACGCAGTTGACGAAACGGCTGAAAAATGCTG
CGGCGAATGTTCTGCGTGAAACTTGGCTCATTGCAAACATAACAAGACTAGTAAAACGG
GTTAATCCCGGCCGTGTAAGAACCCACCAAAGAAAGTTCCTTCTAGCTATATATGCGTT
GCGAAAAGTTAAAATGGATCAGCGCAAACCTAATGGATAATGCAAACACAATAACTGACA
TGGCTAAGACACAAAACACGGTCTACGAGATAATATCGGACATGTCTAGCCGTCAGGAT
GCCATCGAAGAGCGTTTAAACCAACCTACAGGACAAAATGCAGAGCATAACAAGAGCAT
GGAAAGCCTTCCAGACCTATTGTCTCGATGTCTGACCCAGCACCAGGAGCGGATCGAGC
AGCGGCGGAACTTTTTACATCCTGACACAGCTGCAGTTGCCCCCATTC AAGCGCCAACG
CCCCAATCGATGTTCAATGCACCGCCCATGCTGTTTCCACATTCTAGAAGTGTTCCCTC
ATCCAATAACGCCGCTGGTACTTACCATTGGCCAACAAGCCCTATTTTGCCACCTATAT
CTAGTAGAACACCACATTTAGTGCCTGATACTCACATGCCATCAAATGGATCTGCAGTT
AATAGCTACGCATCTTCCAACAAATACGGCAGCTGA

Item D) The nucleotide sequence of several splice variants isolated by 3' race is given below. Sequences begin with exon 12.

Short 13:

GAGCACATGGAAAGCCTTCCAGACCTATTGTCTCGATGTCTGACCCAGCACCAGGAGCG
GATCGAGCAGCGGCGGAACTTTTTACATCCTGACACAGCTGCAGTTGCCCCCATTC AAG
CGCCAACGCCCAATCGATGTTCAATGCAGCGCCCATGCTGTTTCCACATTCTAGTTAA
TAGCTACGCATCTTCCAACAAATACGGCAGCTGAATATCAGAAAGAGAGCGCTCCAAC
CCGTGATTAACATCGAGATGCTAACAATAAGGCCGGATCGATTCTGGCCAACCTCATTC
GCACCC

No 13a:

GAGCACATGGAAAGCCTTCCAGACCTATTGTCTCGATGTCTGACCCAGCACCAGGAGCG
GATCGAGCAGCGGCGGAACTTTTTACATCCTGACACAGCTGCAGTTGCCCCCATTC AAG
CGCCAACGCCCAATCGATGTTCAATGCAGCGCCCATGCTGTTTCCACATTCTAGCGAA
TCGTAGAGCTCAAGGGTACTTCGAGAATCATGCTTCAACAACCGTAACTCTTCTAGCC
AAACCAGGTCCAATAGAACATACATATGTATGTACATACGTGTGTATGTATAGCCAGT

CAATGCCAATGCTAATGAAGAACTGGATTTCGTGTTTTTCGAAAACGTTTCGAACCGGATT
GTGACGAAGCAGCCATTTTGGTGTATTTACACGATAGAATCTAGAAATGGGTCCTTCTC
CCAAAAATATCCCCAC

No 13b:

GAGCACATGGAAAGCCTTCCAGACCTATTGTCTCGATGTCTGACCCAGCACCAGGAGCG
GATCGAGCAGCGGCGGAACTTTTTACATCCTGACACAGCTGCAGTTGCCCCCATTTCAAG
CGCCAACGCCCAATCGATGTTCAATGCAGCGCCCATGCTGTTTCCACATTCTAGCTGA
ATATCAGAAAGAGAGCGCTCCAACCTCCGTGATTAACATCGAGATGCTAACAATAAGGCC
GGATCGATTCTGGCCAACCTCATTTCGCACCCC

Long 13:

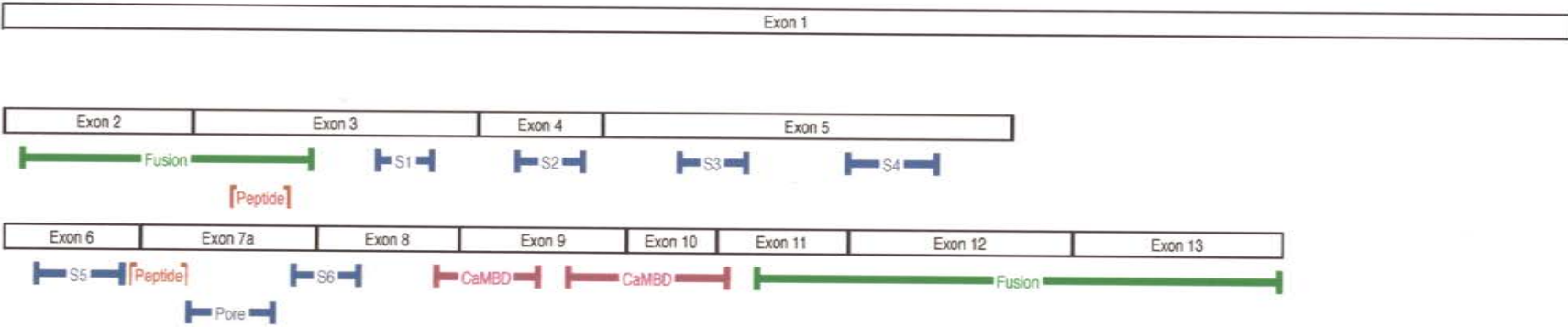
GAGCACATGGAAAGCCTTCCAGACCTATTGTCTCGATGTCTGACCCAGCACCAGGAGCG
GATCGAGCAGCGGCGGAACTTTTTACATCCTGACACAGCTGCAGTTGCCCCCATTTCAAG
CGCCAACGCCCAATCGATGTTCAATGCAGCGCCCATGCTGTTTCCACATTCTAGAAGT
GTTCCCTCATCCAATAACGCCGCTGCTACTTACCATTGGCCAACAAGCCCTATTTTTGCC
ACCTATATCTAGTAGAACACCACATTTAGTGCCTGATACTCACATGCCATCAAATGGAT
CTGCAGTTAATAGCTACGCATCTTCCAACAAATACGGCAGCTGAATATCAGAAAGAGAG
CGCTCCAACCTCCGTGATTAACATCGAGATGCTAACAATAAGGCCGGATCGATTCTGGCC
AACCTCATTTCGCACCCC

Item E) dSK-myc nucleotide sequence with the triple myc tag
sequence indicated in **bold** text:

ATGGCCATTTGCATATCGAACTCGGCCCTGCCGCAGCAGCAGCAGTTGCAGCAACAGTA
TCACCTGCAACAGCAGCAGCAGCACTATCAGTTGCAGCAACACCATCTGCATCAGCAGC
AACTGCAGCAGTCGCAGCAGCAGGTGCCGCGGTGCTAATCACATCATCGCCAACGAAT
GGATCACGGATAATACGGCAAAGTTCACAGCCGGAATCGAGCAGCAGGCCATTTGTTG
TGGTCCCCATTCCGCTTGCCTTGGCCACGCCACTCGCACTCGCACACGGTACCGAATG
TTTCGCTGAAGCAGCTGCGCGAGAGTTCCGGCGATGGAATCGCGGGCATTGCAGCCGAC
TCCCTGCGGATCAACGGTGGCATGCGGCCATTCAAGCAGCTCCGCAAACGGCGTCCGAC
ACTCTCAATTCCTGGCTCGATGAAAACACCTTCCATTGCGAACCGGGAACAGATCTCAT
CTGGATGCAACGAAGAAGCGGCCGAGGCACTAGTGGGTATCCACTCAGACTACCCTAGG
TATGAAATGTATATGGAAGAACGTGCTCTTACTGGCGGCAATACGTCCAGGAAGCCATC
AACAACTCGGCCAAACACAAACCCAATGTGGGCTATCGCCTGGGAAAGAGGAAAGCCC
TCTTCGAGAAGCGCAAACGGATCAGCGATTACGCCCTGGTCATGGGCATGTTCCGGGATC
ATCGTGATGGTTATCGAAAACGAACTGAGCAGTGCCGGTGTCTACACAAAGGCATCGTT
CTACTCGACAGCGTTAAAAACCTTAATATCTGTTTCGACTGTGATTCTTTTAGGACTTA
TAGTAGCTTACCATGCTTTGGAAGTGCAGTTATTCATGATAGATAACTGCGCTGACGAT
TGGAGGATCGCAATGACATGGCAACGAATTAGTCAAATAGGGTTAGAACTTTTTTATATG
CGCTATACATCCAATTCCTGGCGAATACTATTTCCAGTGGACGACGAAATGGCCAATA
AGAAT**GGGCCCGAACAAAACTCATCTCAGAAGAGGATCTGGAACAAAACTCATCTCA
GAAGAAGACTTAGAACAAAACTCATCTCAGAAGAGGATCTGGGGCCCAAACAATTGG
CACCGAAATGGTGCCATATGACGTAGCTTTATCATTACCTATGTTCCCTTCGATTATATT
TAATCTGCCGCGTAATGCTGCTGCATTCAAAGCTATTCACAGATGCATCATCACGGAGC
ATTGGCGCTCTCAATAGGATTAATTTTAAACAAGATTTCGTTTTAAAACTTAATGAC
AATATGTCCGGGAACGGTTCATTGGTCTTCATGGTCTCGCTGTGGATCATCGCATCGT
GGACGCTGCGTCAAGTGCAGAAAGGTTCCACGATGAGGAGCACGCGAATTTGCTAAACTCC**

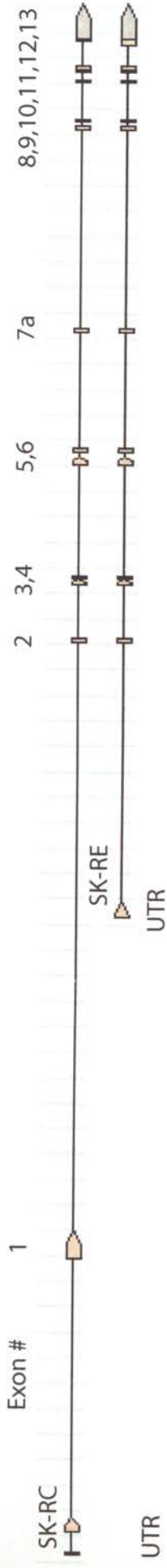
ATGTGGCTAACGGCCATCACATTTCTGTGTGTCTGGCTACGGCGACATTGTGCCAAACAC
GTA CTGTGGACGCGGTATCACCTCACCTGCGGCATGGTGGGCGCCGGCTGTACGGCTC
TACTGGTGGCCGTAGTCTCTCGGAAACTGGAGCTGACCCGTGCTGAGAAGCATGTGCAC
AACTTCATGATGGACACGCAGTTGACGAAACGGCTGAAAAATGCTGCGGCGAATGTTCT
GCGTGAAACTTGGCTCATTGCAAACATAACAAGACTAGTAAAACGGGTTAATCCCGGCC
GTGTAAGAACCCACCAAAGAAAGTTCCTTCTAGCTATATATGCGTTGCGAAAAGTTAAA
ATGGATCAGCGCAAATAATGGATAATGCAAACACAATAACTGACATGGCTAAGACACA
AAACACGGTCTACGAGATAATATCGGACATGTCTAGCCGTGAGGATGCCATCGAAGAGC
GTTTAACCAACCTACAGGACAAAATGCAGAGCATAACAAGAGCACATGGAAAGCCTTCCA
GACCTATTGTCTCGATGTCTGACCCAGCACCAGGAGCGGATCGAGCAGCGGCGGAACTT
TTTACATCCTGACACAGCTGCAGTTGCCCCATTCAAGCGCCAACGCCCCAATCGATGT
TCAATGCACCGCCCATGCTGTTTCCACATTCTAGAAGTGTTCCCTCATCCAATAACGCC
GCTGGTACTTACCATTGGCCAACAAGCCCTATTTTGCCACCTATATCTAGTAGAACACC
ACATTTAGTGCCTGATACTCACATGCCATCAAATGGATCTGCAGTTAATAGCTACGCAT
CTTCCAACAAATACGGCAGCTGA

Appendix Figure A: dSK cDNA cartoon showing the location of peptide and fusion protein epitopes used for the generation of antibodies discussed in the text.



Appendix Figure A

Appendix Figure B: Scale cartoon of the dSK gene showing representative members of the two major dSK transcript classes. One class begins with exon 1 and the associated UTR, and the other class begins with exon 2 and the associated UTR. Within each the two major transcript classes there are variants that contain pore exon 7a or 7b. Additionally there are variants that have differences in exon 13 and the 3' UTR.



Appendix Figure B